BAW-2192
DECEMBER 1993

THE B&W OWNERS GROUP

MATERIALS COMMITTEE

LOW UPPER-SHELF TOUGHNESS FRACTURE ANALYSIS OF REACTOR VESSELS OF B&W OWNERS GROUP REACTOR VESSEL WORKING GROUP

FOR LOAD LEVEL A & B CONDITIONS

B&W NUCLEAR TECHNOLOGIES

BAW-2192

December 1993

LOW UPPER-SHELF TOUGHNESS FRACTURE ANALYSIS OF REACTOR VESSELS OF B&W OWNERS GROUP REACTOR VESSEL WORKING GROUP

FOR LOAD LEVEL A & B CONDITIONS

by

K. K. Yoon

for

B&W Owners Group Materials Committee
Reactor Vessel Working Group
Commonwealth Edison Company
Duke Power Company
Entergy Operations
Florida Power Corporation
Florida Power & Light Company
GPU Nuclear Corporation
Rochester Gas & Electric Corporation
Toledo Edison Company
Virginia Power Company
Wisconsin Electric Power Company

B&W Document No. 77-2192-00

B&W Nuclear Service Company
Engineering and Plant Services Division
P. O. Box 10935
Lynchburg, Virginia 24506-0935

CONTENTS

Contents (Cont'd)

List of Tables

Tables (Cont'd)

List of Figures

Figures (Cont'd)

1. INTRODUCTION

The B&W Owners Group has performed two lead plant fracture mechanics analyses of reactor vessels with low upper-shelf toughness for level A and B service loads. The first analysis, for Turkey Point Units 3 and 4 (BAW-2118P)[1]*, was submitted to the NRC in November 1991 and the second analysis, for Zion Units 1 and 2 (BAW-2148P)[2], was submitted in September 1992. An additional fracture mechanics analysis for level C and D service loads was carried out for all reactor vessels of the B&W Owners Group (B&WOG) Reactor Vessel Working Group (RVWG) and submitted to the NRC in February 1993 (BAW-2178P)[3].

By a letter addressed to the NRC[4] in 1992, the B&WOG RVWG stated that the second lead plant analysis for the Zion Units bounds the B&W fabricated PWR vessels. This report documents an analysis showing that all B&W fabricated PWR vessels are bounded by the lead plant analysis of reference 2 for level A and B service loads.

The B&WOG RVWG is composed of the owners of seven B&W-designed 177-FA units and nine Westinghouse NSSS with B&W fabricated reactor vessels. The B&WOG RVWG member utilities and their plants are listed in Table 1-1. All these reactor vessels were fabricated by B&W and contain Mn-Mo-Ni/Linde 80 ASA weld metals. This group has been working together to conduct shared research and development projects to address reactor vessel integrity issues for their vessels and share materials data through the Master Integrated Reactor Vessel Surveillance Program described earlier in references 1 and 2, in addition to each plant's plant-specific surveillance program.

---

*Number designates reference in section 7.

Table 1-1. B&W Owners Group RVWG Plants

Utility	Plant
Entergy Operations, Inc.	ANO-1
Commonwealth Edison Company	Zion 1 and 2
Duke Power Company	Oconee 1, 2, and 3
Florida Power Corporation	Crystal River-3
Florida Power & Light Company	Turkey Point 3 and 4
GPU Nuclear Corporation	Three Mile Island-1
Rochester Gas & Electric	R. E. Ginna
Toledo Edison Company	Davis-Besse-1
Virginia Power Company	Surry 1 and 2
Wisconsin Electric Power Company	Point Beach 1 and 2

2. FRACTURE MECHANICS ANALYSIS METHODOLOGY

The minimum Charpy upper-shelf energy requirement is in Title 10, Code of Federal Regulations, Part 50, Appendix G, i.e. a Charpy upper-shelf energy must be maintained at no less than 50 ft-lbs. If any of the pressure boundary materials does not comply with these requirements then a supplemental fracture mechanics analysis is required to assure the reactor coolant pressure boundary integrity. The only area of the reactor coolant boundary which has any likelihood to fall below the 50 ft-lbs level i the reactor vessel beltline region. The evaluation described in this report is restricted to the beltline region.

The ASME Boiler and Pressure Vessel Code, Section XI, Appendix G, contains operating guidelines for the prevention of nonductile failure. Since fracture toughness is a function of temperature, this requirement forces that the pressure boundary components be operated at a sufficiently low pressure as to preclude non-ductile failure. However, in the high operating temperature regime, ductile tearing is the expected fracture mode for ferritic reactor vessel materials. The current specifications in ASME Section XI, Appendix G, do not provide guidance in preventing ductile failures, implying that the nonductile failure limit would conservatively cover the ductile failure mode. Recently, the Working Group on Flaw Evaluation of Section XI of the ASME Boiler and Pressure Vessel Code Committee recognized that at the upper-shelf temperature range there is no longer a concern over cleavage type failures and established a new and separate set of acceptance criteria solely for the upper-shelf temperature region. Evaluation for ductile fracture may be performed by a J-integral based elastic-plastic fracture mechanics method.

2.1. Acceptance Criteria

The following acceptance criteria were developed by an industry consensus group, the Working Group on Flaw Evaluation of the ASME Boiler and Pressure Vessel Committee's Subcommittee on Nuclear Inservice Inspection[5]. This was published in Code Case N-512[6] and will be further implemented as a Nonmandatory Appendix[7] to Section XI of the Boiler and Pressure Vessel Code.

Article X-2000
Acceptance Criteria

2.1.1. X-2100 Scope

Adequacy of the upper-shelf toughness of the reactor vessel shall be determined by analysis. The reactor vessel is acceptable for continued service when the criteria of X-2200, X-2300, and X-2400 are satisfied.

2.1.2. X-2200 Level A and B Service Loadings

(a) When evaluating adequacy of the upper-shelf toughness for the weld material for Level A and B Service Loadings, an interior semi-elliptical surface flaw with a depth one-quarter of the wall thickness and a length six times the depth shall be postulated, with the flaw's major axis oriented along the weld of concern, and the flaw plane oriented in the radial direction. When evaluating adequacy of the upper-shelf toughness for the base material, both interior axial and circumferential flaws with depths one-quarter of the wall thickness and lengths six times the depth shall be postulated, and toughness properties for the corresponding orientation shall be used. Smaller flaw sizes may be used when justified. Two criteria shall be satisfied:

(1) The applied J-integral evaluated at a pressure 1.15 times the accumulation pressure as defined in the plant-specific Overpressure Protection Report, with a factor of safety of 1.0 on thermal loading for the plant-specific heatup and cooldown conditions, shall be less than the J-integral of the material at a ductile flaw extension of 0.10 in.

(2) Flaw extensions at pressures up to 1.25 times the accumulation pressure of X-2200 (a-1) shall be ductile and stable, using a factor of safety of 1.0 on thermal loading for the plant-specific heatup and cooldown conditions.

(b) The J-integral resistance versus flaw extension curve shall be a conservative representation for the vessel material under evaluation.

2.1.3. X-2300 Level C Service Loadings

(a) When evaluating adequacy of the upper-shelf toughness for the weld material for Level C Service Loadings, interior semi-elliptical surface flaws with depths up to 1/10 of the base metal wall thickness, plus the cladding thickness, with total depths not exceeding 1.0 in., and a surface length six times the depth, shall be postulated, with the flaw's major axis oriented along the weld of concern, and the flaw plane oriented in the radial direction. When evaluating adequacy of the upper-shelf toughness for the base material, both interior axial and circumferential flaws shall be postulated, and toughness properties for the corresponding orientation shall be used. Flaws of various depths, ranging up to the maximum postulated depth, shall be analyzed to determine the most limiting flaw depth. Smaller maximum flaw sizes may be used when justified. Two criteria shall be satisfied:

(1) The applied J-integral shall be less than the J-integral of the material at a ductile flaw extension of 0.10 in., using a factor of safety of 1.0 on loading.

(2) Flaw extensions shall be ductile and stable, using a factor of safety of 1.0 on loading.

(b) The J-integral resistance versus flaw extension curve shall be a conservative representation for the vessel material under evaluation.

2.1.4. X-2400 Level D Service Loadings

(a) When evaluating adequacy of the upper-shelf toughness for Level D Service Loadings, flaws as specified for Level C Service Loadings in X-2300 shall be postulated, and toughness properties for the corresponding orientation shall be used. Flaws of various depths, ranging up to the maximum postulated depth, shall be analyzed to determine the most limiting flaw depth. Smaller maximum flaw sizes may be used when justified. Flaw extensions shall be ductile and stable, using a factor of safety of 1.0 on loading.

(b) The J-integral resistance versus flaw extension curve shall be a best-estimate representation for the vessel material under evaluation.

(c) The extent of stable flaw extension shall be less than or equal to 75% of the vessel wall thickness, and the remaining ligament shall not be subject to tensile instability.

2.2. Elastic-Plastic Fracture Mechanics Methods

In references 1 and 2, the J-integral based elastic-plastic fracture mechanics methods were described and used for the evaluation of the Zion and Turkey Point vessels (See Appendix A to this report). After completion of these two analyses, the ASME B&PV Committee Code Case N-512 which contains the acceptance criteria and simplified methodology and is working on a proposed Appendix.

In this report, the B&W Owners Group methods described in Appendix A are used because (1) these methods were used in reference 1 and 2; (2) the NRC staff has already reviewed references 1 and 2; and (3) these methods differ little from the methods of Code Case N-512.

3. MATERIAL PROPERTIES

3.1. J-Resistance Model for Mn-Mo-Ni/Linde 80 Welds

The J-resistance model for Mn-Mo-Ni/Linde 80 welds in the reactor vessels of the RVWG plants were developed using a large J-resistance data base and used in reference 1 and 2. A detailed description of this model is provided in Appendix B of this report.

The final form of this model is presented as follows:

$$J = C1\ (\Delta a)^{C2} \exp(C3\ \Delta a^{C4}) \tag{3-1}$$

where

$$\ell n\ C1 = a1 + a2\ \ Cu(\phi t)^{a7} \ \ + a3\ T + a4\ \ell n\ B_N \tag{3-2}$$

$$C2 = d1 + d2\ \ell n\ C1 + d3\ \ell n\ B_N \tag{3-3}$$

$$C3 = d4 + d5\ \ell n\ C1 + d6\ \ell n\ B_N \tag{3-4}$$

where

T - temperature in F

ϕt - fluence, 10^{-18} n/cm^2

B_N - net specimen thickness in inches.

All a and d coefficients are provided in Table 3-1.

3.2. Mechanical Properties of Weld Metals

The following irradiated mechanical properties of reactor vessel weld metals are used for this evaluation. These properties are the same as those in reference 2.

Yield Strength σ_y = 85.1 ksi

Ultimate Strength σ_{ult} = 100.65 ksi

Young's Modulus E = 26,975 ksi

Ramberg-Osgood Constants

α = 1.56

n = 8.34.

Table 3-1. Parameters in J_D Model

a1 a2 a3 a4 a7	
d1 d2 d3 d4 d5 d6	
# of points SIG () ^2 in ln(J) Se in ln(J) Se in log(J)	
Ratio -1 Se -2 Se	

4. REACTOR VESSELS OF B&W OWNERS REACTOR VESSEL WORKING GROUP

Plant-specific mechanical and fracture toughness properties of reactor pressure vessels are essential. Plant specific data needed for the analyses are provided in Table 4-1. Fluences are based on 32 EFPY or the end of the license period for each plant. Location of reactor vessel welds for each of the B&WOG RVWG member plant vessels are shown in Appendix C.

Table 4-1. End-of-Life (32 EFPY) Fluence Predictions for Beltline Region Weld of B&W Fabricated Reactor Vessels

Plant	Weld Location	Weld Number	Cu (wt%)	Ni (wt%)	Fluence (n/cm^2)		Reference
					IS	T/4	
Oconee Unit 1	NB/IS	SA-1135	0.25	0.54	1.18E+18	6.61E+17	BAW-2108,R1
	IS/US	SA-1229, 61% ID	0.26	0.61	7.96E+18	4.46E+18	
		WF-25, 39% OD	0.35	0.68	---	---	
	US/LS	SA-1585	0.21	0.59	8.68E+18	4.86E+18	
	LS/Dutch.	WF-9	0.21	0.59	5.06E+16	2.83E+16	
	IS Long.	SA-1073	0.21	0.64	6.28E+18	3.52E+18	
	US Long.	SA-1493	0.20	0.55	7.23E+18	4.05E+18	
	LS Long.	SA-1430	0.20	0.55	7.29E+18	4.08E+18	
		SA-1426	0.20	0.55	7.29E+18	4.08E+18	
Oconee Unit 2	NB/US	WF-154	0.31	0.59	8.42E+18	4.72E+18	BAW-2108,R1
	US/LS	WF-25	0.35	0.68	9.19E+18	5.15E+18	
	LS/Dutch	WF-112	0.31	0.59	5.36E+16	3.00E+16	
Oconee Unit 3	NB/US	WF-200	0.24	0.63	8.26E+18	4.63E+18	BAW-2108,R1
	US/LS	WF-67, 75% ID	0.24	0.60	9.01E+18	5.05E+18	
		WF-70, 25% OD	0.35	0.59	---	---	
	LS/Dutch	WF-169-1	0.18	0.63	5.26E+18	2.95E+16	
Three Mile Island Unit 1	NB/US	WF-70	0.35	0.59	7.89E+18	4.42E+18	BAW-2108,R1
	US/LS	WF-25	0.35	0.68	8.61E+18	4.82E+18	
	LS/Dutch	WF-67, 50% ID	0.24	0.60	5.02E+16	2.81E+16	
		WF-70, 50% OD	0.35	0.59	---	---	
	US Long.	WF-8	0.20	0.55	8.97E+18	5.02E+18	
	LS Long.	SA-1526	0.35	0.68	7.76E+18	4.35E+18	
		SA-1526, 37% ID	0.35	0.68	7.76E+18	4.35E+18	
		SA-1494, 63% OD	0.18	0.63	---	---	

End-of-Life (32 EFPY) Fluence Predictions for Beltline
Region Weld of B&W Fabricated Reactor Vessels

Plant	Weld Location	Weld Number	Cu (wt%)	Ni (wt%)	Fluence (n/cm^2)		Reference
					IS	T/4	
Crystal River Unit 3	NB/US	SA-1769, 40% ID	0.26	0.61	7.53E+18	4.22E+18	BAW-2108,R1
		WF-169-1, 60% OD	0.18	0.63	---	---	
	US/LS	WF-70	0.35	0.59	8.22E+18	4.60E+18	
	LS/Dutch	WF-154	0.31	0.59	4.79E+16	2.68E+16	
	US Long.	WF-18	0.20	0.55	7.96E+18	4.46E+18	
		WF-8	0.20	0.55	7.96E+18	4.46E+18	
	LS Long.	SA-1580	0.20	0.55	6.98E+18	3.91E+18	
Arkansas Nuclear One Unit 1	NB/US	WF-182-1	0.24	0.63	8.62E+18	4.83E+18	BAW-2108,R1
	US/LS	WF-112	0.31	0.59	9.40E+18	5.26E+18	
	LS/Dutch	SA-1788	0.25	0.54	5.48E+16	3.07E+16	
	US Long.	WF-18	0.20	0.55	7.05E+18	3.95E+18	
	LS Long.	WF-18	0.20	0.55	6.95E+18	3.89E+18	
Davis-Besse	NB/US	WF-232, 9% ID	0.18	0.64	1.50E+18	---	BAW-2108,R1
		WF-233, 91% OD	0.29	0.68	---	8.40E+17	
	US/LS	WF-182-1	0.24	0.63	1.07E+19	5.99E+18	
	LS/Dutch	WF-232, 12% IS	0.18	0.64	6.00E+16	---	
		WF-233, 88% OD	0.29	0.68	---	3.36E+16	
R. E. Ginna	NB/IS	SA-1101	0.26	0.60	3.69E+18	2.71E+18	WCAP-13272
	IS/LS	SA-847	0.25	0.54	3.35E+19	2.46E+19	
	LS/Dutch	SA-848	0.25	0.54	---	---	

End-of-Life (32 EFPY) Fluence Predictions for Beltline
Region Weld of B&W Fabricated Reactor Vessels

Plant	Weld Location	Weld Number	Cu (wt%)	Ni (wt%)	Fluence (n/cm^2)		Reference
					IS	T/4	
Point Beach Unit 1	NB/IS	SA-1426	0.20	0.55	3.17E+18	2.33E+18	WCAP-12794, R2
	IS/LS	SA-1101	0.26	0.60	2.43E+19	1.78E+19	
	LS/Dutch	SA-1101	0.26	0.60	---	---	
	IS Long.	SA-812, 27% ID	0.17	0.52	1.78E+19	1.32E+19	
		SA-775, 73% OD	0.19	0.63	---	---	
	LS Long.	SA-847	0.25	0.54	1.63E+19	1.21E+19	
Point Beach Unit 2	NB/IS	CE/SAW	0.27	0.90	3.70E+18	2.72E+ 18	WCAP-12795, R2
	IS/LS	SA-1484	0.24	0.60	2.52E+19	1.85E+19	
	LS/Dutch	CE/SAW	---	---	---	---	
Surry Unit 1	NB/IS	J726	0.33	0.10	5.27E+18	2.64E+18	WCAP-11015, R1
	IS/LS	SA-1585, 40% ID	0.21	0.59	4.39E+19	2.20E+19	
		SA-1650, 60% OD	0.21	0.59	---	---	
	IS Long.	SA-1494	0.18	0.63	7.08E+18	3.54E+18	
	LS Long.	SA-1494	0.18	0.63	7.08E+18	3.54E+18	
		SA-1526	0.35	0.68	7.08E+18	3.54E+18	
Surry Unit 2	NB/IS	L737	0.35	0.10	4.45E+18	2.23E+18	WCAP-11015, R1
	IS/LS	R3008	0.19	0.56	3.71E+19	1.86E+19	
	IS Long.	SA-1585	0.21	0.59	7.75E+18	3.88E+18	
		SA-1585, 50% ID	0.21	0.59	7.75E+18	3.88E+18	
		WF-4, 50% OD	0.20	0.55	---	---	
	LS Long.	WF-4	0.20	0.55	7.75E+18	3.88E+18	
		WF-4, 63% ID	0.20	0.55	7.75E+18	3.88E+18	
		WF-8, 37% OD	0.20	0.55	---	---	

End-of-Life (32 EFPY) Fluence Predictions for Beltline
Region Weld of B&W Fabricated Reactor Vessels

Plant	Weld Location	Weld Number	Cu (wt%)	Ni (wt%)	Fluence (n/cm^2)		Reference
					IS	T/4	
Turkey Point Unit 3	NB/IS	SA-1484	0.24	0.60	3.30E+18	1.98E+18	Turkey Point Units 3 & 4 Docket Nos. 50-250 & 50-251 10CFR50.61 Report
	IS/LS	SA-1101	0.26	0.60	2.64E+19	1.58E+19	
	LS/Dutch	SA-1135	0.25	0.54	---	---	
Turkey Point Unit 4	NB/IS	WF-67, 67% ID	0.24	0.60	3.16E+18	1.90E+18	Turkey Point Units 3 & 4 Docket Nos. 50-250 & 50-251 10CFR50.61 Report
		WF-70, 33% OD	0.35	0.59	---	---	
	IS/LS	SA-1101	0.26	0.60	2.53E+19	1.52E+19	
	LS/Dutch	SA-1135	0.25	0.54	---	---	
Zion Unit 1	NB/IS	WF-154, 82% ID	0.31	0.59	1.21E+19	6.53E+18	WCAP-10962, R3
		SA-1769, 18% OD	0.26	0.61	---	---	
	IS/LS	WF-70	0.35	0.59	1.73E+19	9.34E+18	
	LS/Dutch	WF-154	0.31	0.59	---	---	
	IS Long.	WF-4	0.20	0.55	6.29E+18	3.40E+18	
		WF-8, 39% ID	0.20	0.55	6.29E+18	3.40E+18	
		WF-4, 61% OD	0.20	0.55	---	---	
	LS Long.	WF-8	0.20	0.55	6.29E+18	3.40E+18	

End-of-Life (32 EFPY) Fluence Predictions for Beltline
Region Weld of B&W Fabricated Reactor Vessels

Plant	Weld Location	Weld Number	Cu (wt%)	Ni (wt%)	Fluence (n/cm^2)		Reference
					IS	T/4	
Zion Unit 2	NB/IS	WF-200	0.24	0.63	1.30E+19	7.02E+18	WCAP-10962, R3
	IS/LS	SA-1769	0.26	0.61	1.69E+19	9.13E+18	
	LS/Dutch	WF-154	0.31	0.59	---	---	
	IS Long.	WF-70	0.35	0.59	6.04E+18	3.26E+18	
	LS Long.	WF-29	0.23	0.63	6.04E+18	3.26E+18	

5. FRACTURE MECHANICS ANALYSIS

5.1. Plant Operation Data

Plant-specific and operational data for all sixteen plants are listed in Table 5-1. The loads considered in this evaluation are due to internal pressure and thermal gradient loads. The accumulation pressure is taken as ten percent above the design pressure:

$P_{acc.} = 1.1 \times P_{design}$

For $P_{design} = 2485$ psi $P_{acc.} = 2734$ psi

For $P_{design} = 2500$ psi $P_{acc.} = 2750$ psi

In accordance with acceptance criteria, the following pressures are to be applied:

Criterion #1

$P = 1.15\ P_{acc.}$

Criterion #2

$P = 1.25\ P_{acc.}$ for stability check.

5.2. Plant-Specific Material Properties

The beltline region welds and their estimated fluence levels at 32 EFPY are given in Table 4-1 and the operating temperatures for each plant are listed in Table 5-1. Using these input data and the B&WOG J-R model described in section 3, the weld metal specific material J-R values can be calculated. Based on the J-R values, most likely limiting welds for each reactor vessels are shown in Table 5-2.

5.3. Stress Intensity Factor for Thermal Loading

In references 1 and 2, the stress intensity factors due to thermal gradient loading, K_{IT}, were calculated by BWNT computer program PTPC[8] which is based on a quarter thickness infinite flaw. However, since ASME B&PV Code, Section XI proposed a K_{IT} equation for semielliptical surface flaws (which received extensive verification including material property sensitivity study) the proposed code equation [9] is used for this evaluation as follows:

$$K_{IT} = 0.001 \text{ (CR) } t^{2.5} F_3 \text{ , ksi}\sqrt{\text{in}}$$

where

CR - cooldown rate

t - thickness of vessel

$$F_3 = 0.617 + 2.795 \text{ (a/t)} - 6.646 \text{ (a/t)}^2 + 3.157 \text{ (a/t)}^3$$

The values for a cooldown rate of 100 degree F per hour are listed in Table 5-3. A significant portion of the thermal gradient load would be relieved at the onset of ductile tearing. However, in this analysis, this fact is ignored and the K_{IT}, as calculated, is conservatively included as a primary load.

5.4. J Analysis

For Acceptance Criterion #1, an applied J must be calculated at a flaw size equal to the wall quarter-thickness plus a flaw extension of 0.1 inch:

$$a = a_o + \Delta a = t/4 + 0.1$$

To conservatively combine pressure and thermal gradient stresses, the following approach is used for applied J calculation:

$$J = J^E + J^P$$

$$= [K_I(a_e, p) + K_{IT}]^2/E'.$$

For definitions of the terms in these equations, see Appendix A.

Equation A-2 was used for K_I for a longitudinal semielliptical surface flaw and equation A-7 for a circumferential flaw. Since the plastic part of J, J^P, is very small compared with J^E, the J^P term can be disregarded at this pressure level.

For the first acceptance criterion, the applied J values are calculated using a pressure load of 1.15 times the accumulation pressure and the thermal gradient loading. These are listed in Table 5-3 along with the J-R values at Δa equal to 0.1 inch. Ratios between these two columns of J values are also listed in the table. All of these ratios are greater than one, it may therefore conclude that the first acceptance criterion is met for all the RVWG plant reactor vessels. The acceptance criterion includes the required safety margins. In reference 2, a longitudinal reference flaw was analyzed for the circumferential weld in Zion Unit 1 vessel which has high fluence and copper content combination. Therefore, the results shown in reference 2 bounded the remainder of the B&WOG RVWG plant vessels.

5.5. Stability Analysis

The stability analysis is performed using the J-Δa method. The second criterion requires that the combined loads of (1) pressure of 1.25 P_{acc} and (2) thermal gradient should be less than the instability load. Conversely, it can be shown that the combined load is stable. In Table 5-3, a second column of applied Js is shown that were generated using a pressure of 1.25 times the accumulation pressure and the thermal loading. Ratios between the material $J_{0.1}$ and these applied J columns is also given. All these ratios are greater than unity indicating that the material J-R values are higher than the applied J values at $\Delta a = 0.1$ inch and the material J-R curve and the applied J curve intersected at $\Delta a < 0.1$ inch point. To complete the stability check, the slope of the material curve must be steeper than that of the applied J curve. This is demonstrated in Figure 5-1 which was reported in reference 2 for the Zion Units 1 and 2 analysis. The remainder of the J-R curves and the applied J curves are similar to Figure 5-1. Therefore, the second acceptance criterion is satisfied.

Table 5-1. Reactor Vessel Dimensions and Operating Conditions

Group	Plant	Ri (in)	t (in)	Design Pressure (psi)	Cold Leg Temp. (F)
B&W NSSS	Oconee-1	85.5	8.44	2500	556
	Oconee-2	85.5	8.44	2500	556
	Oconee-3	85.5	8.44	2500	556
	TMI-1	85.5	8.44	2500	556
	Crystal River-3	85.5	8.44	2500	556
	ANO-1	85.5	8.44	2500	556
	Davis-Besse	85.5	8.44	2500	556
W NSSS	R. E. Ginna	66	6.5	2485	546
	Point Beach-1	66	6.5	2485	542
	Point Beach-2	66	6.5	2485	542
	Surry-1	78.5	7.75	2485	543
	Surry-2	78.5	7.75	2485	543
	Turkey Point-3	77.75	7.75	2485	546
	Turkey Point-4	77.75	7.75	2485	546
	Zion-1	86.5	8.44	2485	529
	Zion-2	86.5	8.44	2485	529

All data from BAW-1543, Rev. 4.[10]

Table 5-2. Controlling Weld Metals in RVWG Reactor Vessels

Plant	Cold Leg Temp. (F)	Controlling Welds				Fluence x E-18 (n/cm^2)		Lower Bounding J-R($J_{0.1}$) (lb/in)
		Weld Number	Weld Orien*	Cu (w%)	Ni (w%)	I.S.	t/4	
Oconee-1	556	SA-1229	C	0.26	0.61	7.96	4.46	625
	556	SA-1585	C	0.21	0.59	8.68	4.86	665
	556	SA-1430	L	0.20	0.55	7.29	4.08	677
Oconee-2	556	WF-25	C	0.35	0.68	9.19	5.15	552
Oconee-3	556	WF-67	C	0.24	0.60	9.01	5.05	638
TMI-1	556	WF-25	C	0.35	0.68	8.61	4.82	554
	556	SA-1526	L	0.35	0.68	7.76	4.35	558
CR-3	556	WF-70	C	0.35	0.59	8.22	4.60	556
	556	WF-8, WF-18	L	0.20	0.55	7.96	4.46	675
ANO-1	556	WF-182-1	C	0.24	0.63	8.62	4.83	639
	556	WF-112	C	0.31	0.59	9.40	5.26	581
	556	WF-18	L	0.20	0.55	7.05	3.95	678
Davis Besse	556	WF-182-1	C	0.24	0.63	10.70	5.99	634
R.E. Ginna	546	SA-1101	C	0.26	0.60	3.69	2.71	645
	546	SA-847	C	0.25	0.54	33.50	24.60	593
PB-1	542	SA-1426	C	0.20	0.55	3.17	2.33	699
	542	SA-1101	C	0.26	0.60	24.30	17.80	597
	542	SA-812	L	0.17	0.52	17.80	13.20	691
	542	SA-847	L	0.25	0.54	16.30	12.10	618
PB-2	542	CE/SAW	C	0.27	0.90	3.70	2.72	640
	542	SA-1484	C	0.24	0.60	25.20	18.50	613

Table 5-2. Controlling Weld Metals in RVWG Reactor Vessels (Cont'd)

Plant	Cold Leg Temp. (F)	Controlling Welds				Fluence x E-18 (n/cm^2)		Lower Bounding J-R($J_{0.1}$) (lb/in)
		Weld Number	Weld Orien*	Cu (w%)	Ni (w%)	I.S.	t/4	
Surry-1	543	SA-1585	C	0.21	0.59	43.90	22.00	637
	543	SA-1526	L	0.35	0.68	7.08	3.54	572
Surry-2	543	L737	C	0.35	0.10	4.45	2.23	586
	543	R3008	C	0.19	0.56	37.10	18.60	662
	543	SA-1585	L	0.21	0.59	7.75	3.88	679
TP-3	546	SA-1101	C	0.26	0.60	26.30	15.80	597
TP-4	546	SA-1101	C	0.26	0.60	25.30	15.20	598
Zion-1	529	WF-70	C	0.35	0.59	17.30	9.34	549
	529	WF-8, WF-4	L	0.20	0.55	6.29	3.40	700
Zion-2	529	SA-1769	C	0.26	0.61	16.90	9.13	623
	529	WF-70	L	0.35	0.59	6.04	3.26	583

*Weld Orientation

C - Circumferential
L - Longitudinal

Table 5-3. Acceptance Assessment

Plant	Weld Number	Weld Orientation	Lower Bounding J-R($J_{0.1}$) (lb/in)	Applied J (SF = 1.15)				Applied J (SF = 1.25)	
				KI(T) (ksi)	KI(ae,p) (ksi)	J_{app}(ae) (lb/in)	$J_{0.1}/J_{app}$	J_{app}(ae) (lb/in)	$J_{0.1}/J_{app}$
Oconee-1	SA-1229	C	625	19.7	51.7	173	3.62	196	3.19
	SA-1585	C	665	19.7	51.7	173	3.85	196	3.39
	SA-1429	L	677	19.7	98.5	474	1.43	547	1.24
Oconee-2	WF-25	C	552	19.7	51.7	173	3.20	196	2.82
Oconee-3	WF-67	C	638	19.7	51.7	173	3.70	196	3.26
TMI-1	WF-25	C	554	19.7	51.7	173	3.21	196	2.83
	SA-1526	L	558	19.7	98.5	474	1.18	547	1.02
CR-3	WF-70	C	556	19.7	51.7	173	3.22	196	2.84
	WF-8, WF-18	L	675	19.7	98.5	474	1.43	547	1.23

Table 5-3. Acceptance Assessment (Cont'd)

Plant	Weld Number	Weld Orientation	Lower Bounding J-R($J_{0.1}$) (lb/in)	Applied J (SF = 1.15)				Applied J (SF = 1.25)	
				KI(T) (ksi)	KI(ae,p) (ksi)	J_{app}(ae) (lb/in)	$J_{0.1}/J_{app}$	J_{app}(ae) (lb/in)	$J_{0.1}/J_{app}$
ANO-1	WF-182-1	C	639	19.7	51.7	173	3.70	196	3.27
	WF-112	C	581	19.7	51.7	173	3.37	196	2.97
	WF-18	L	678	19.7	98.5	474	1.43	547	1.24
Davis Besse	WF-182-1	C	634	19.7	51.7	173	3.67	196	3.24
R.E. Ginna	SA-1101	C	645	10.2	45.6	105	6.12	121	5.31
	SA-847	C	593	10.2	45.6	105	5.64	121	4.89
PB-1	SA-1426	C	699	10.2	45.6	105	6.64	121	5.77
	SA-1101	C	597	10.2	45.6	105	5.67	121	4.93
	SA-812	L	691	10.2	86.9	319	2.17	[illegible]	1.86
	SA-847	L	618	10.2	86.9	319	1.94	372	1.66
PB-2	CE/SAW	C	640	10.2	45.6	105	6.08	121	5.28
	SA-1484	C	613	10.2	45.6	105	5.82	121	5.06

Table 5-3. Acceptance Assessment (Cont'd)

Plant	Weld Number	Weld Orientation	Lower Bounding J-R($J_{0.1}$) (lb/in)	Applied J (SF = 1.15)				Applied J (SF = 1.25)	
				KI(T) (ksi)	KI(ae,p) (ksi)	J_{app}(ae) (lb/in)	$J_{0.1}/J_{app}$	J_{app}(ae) (lb/in)	$J_{0.1}/J_{app}$
Surry-1	SA-1585	C	637	15.9	49.4	144	4.43	164	3.88
	SA-1526	L	572	15.9	94.1	409	1.40	474	1.21
Surry-2	L737	C	586	15.9	49.4	144	4.1	164	3.6
	R3008	C	662	15.9	49.4	144	4.60	164	4.03
	SA-1585	L	679	15.9	94.1	409	1.66	474	1.43
TP-3	SA-1101	C	597	15.9	49.0	142	4.20	162	3.68
TP-4	SA-1101	C	598	15.9	49.0	142	4.20	162	3.69
Zion-1	WF-70	C	549	19.7	51.9	173	3.18	196	2.80
	WF-70	L*	549	19.7	99.0	475	1.16	548	1.00
	WF-8, WF-4	L	700	19.7	99.0	475	1.48	548	1.28

Table 5-3. Acceptance Assessment (Cont'd)

Plant	Weld Number	Weld Orientation	Lower Bounding J-R($J_{0.1}$) (lb/in)	Applied J (SF = 1.15)				Applied J (SF = 1.25)	
				KI(T) (ksi)	KI(ae,p) (ksi)	J_{app}(ae) (lb/in)	$J_{0.1}/J_{app}$	J_{app}(ae) (lb/in)	$J_{0.1}/J_{app}$
Zion-2	SA-1769	C	623	19.7	51.9	173	3.61	196	3.18
	WF-70	L	583	19.7	99.0	475	1.23	548	1.06

*A longitudinal flaw was postulated in the WF-70 circumferential weld to lower bound the remainder of the B&W RVWG vessels.

Figure 5-1. J-Δa Plot for Acceptance Criterion #2 for Zion Units 1 and 2

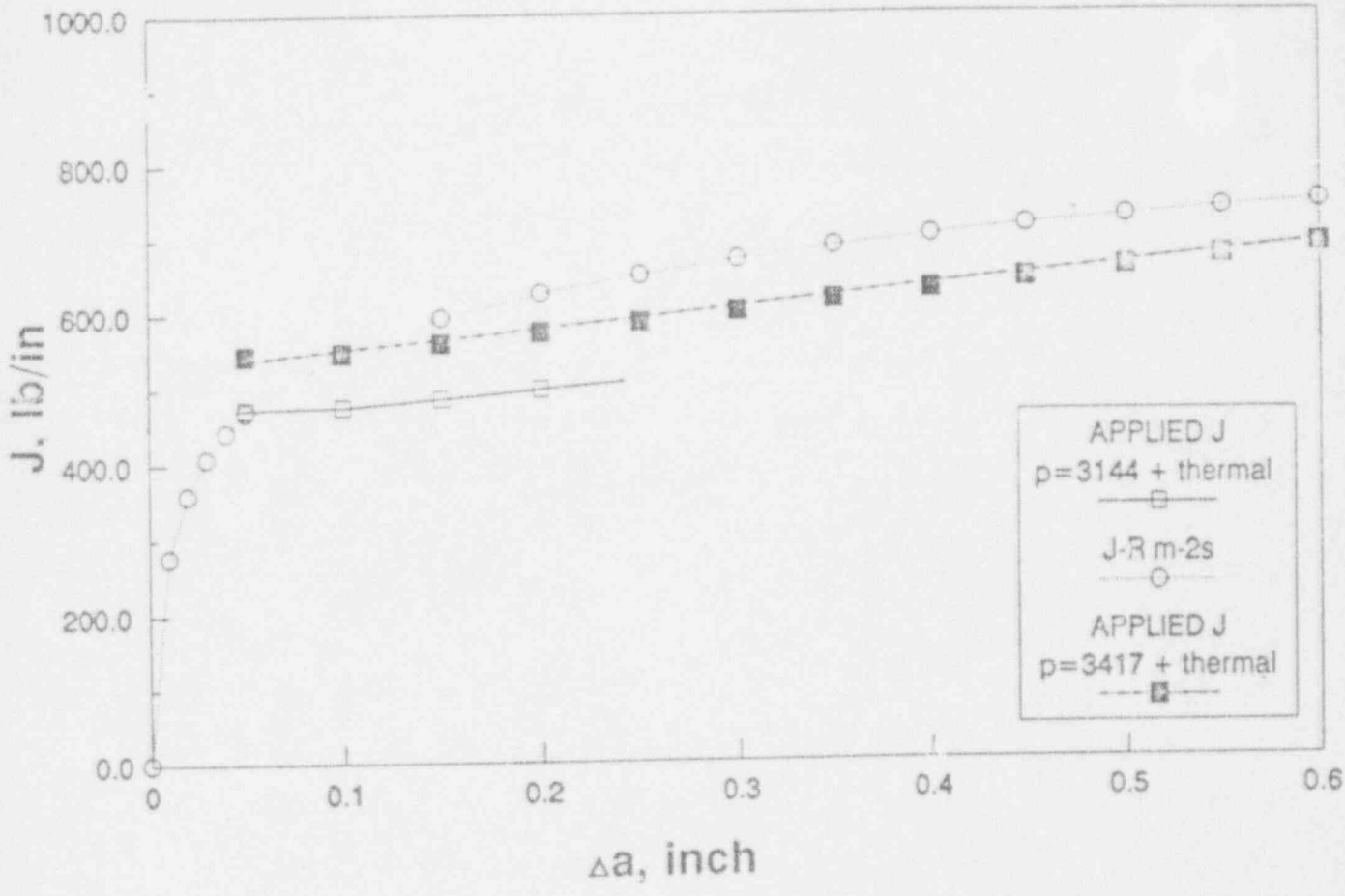

6. SUMMARY AND CONCLUSIONS

Through the B&W Owners Group Integrated Surveillance Program, an extensive J-resistance data base was assembled for over more than fifteen years. This was achieved through a carefully planned, long-term cooperative effort by the affected licensees and B&W Nuclear Technologies. A comprehensive mathematical model for J-resistance behavior of Mn-Mo-Ni/Linde 80 weld metals was developed through application of a state-of-the-art pattern recognition method.

While this data collection was in progress, an industry - NRC consensus effort (through the ASME Boiler and Pressure Vessel Code Committee) produced acceptance criteria for low upper-shelf fracture toughness under A and B load conditions.

The J-integral based elastic-plastic fracture mechanics methodology, developed through NRC regulatory research programs with industry efforts by the B&W Owners Group, EPRI and others, now allows the lower upper-shelf fracture toughness concern to be addressed using the J-resistance model and the acceptance criteria.

This analysis for low upper-shelf fracture toughness concern was performed using very conservative material models and load combination, i.e. treating thermal gradient stress as a primary stress.

The analytical results for the major welds in each reactor vessel of the B&WOG RVWG plants indicate that there are additional margins beyond the required margin built into the acceptance criteria. These additional margins range from 1.23 to 5.82 in terms of J, which is equivalent to 1.10 to 2.4 in terms of loads. This analysis was submitted to the Nuclear Regulatory Commission to demonstrate compliance with 10CFR50, Appendix G.

7. REFERENCES

1. BAW-2118P, Low Upper-Shelf Toughness Fracture Analysis of Reactor Vessels of Turkey Point Units 3 and for Load Level A & B Conditions, B&W Owners Group, November 1991.

2. BAW-2148P, Rev. 1, Low Upper-Shelf Toughness Fracture Analysis of Reactor Vessels of Zion Units 1 and 2 for Load Level A & B Conditions, B&W Owners Group, April 1992.

3. K. K. Yoon, Low Upper-Shelf Toughness Fracture Mechanics Analysis of Reactor Vessels of B&W Owners Reactor Working Group for Level C & D Service Loads, BAW-2178P, B&W Owners Group, February 1993.

4. Letter, from Chairman, B&W Owners Reactor Vessel Working Group to NRC/NRR, "Appendix G Analysis for B&W Owners Group Reactor Vessel Working Group Plants," September 10, 1992.

5. American Society of Mechanical Engineers, Section XI, "Rules for Inservice Inspection of Nuclear Power Plant Components," of ASME Boiler and Pressure Vessel Code, New York (updated frequently).

6. Code Case N-512, "Reactor Vessels with Low Upper Shelf Charpy Energy Levels," ASME Boiler and Pressure Vessel Code, Section XI, 1993.

7. Working Group on Flaw Evaluations, "Draft Appendix 'X' - Reactor Vessels with Low Upper Shelf Charpy Charpy Energy Levels," Revision 13, ASME Boiler and Pressure Vessel Code, Section XI, 1993.

8. B&W Nuclear Service Co., "PTPC-Pressure-Temperature Limit Analysis Program," Version 3.1, March 1990.

9. Committee Correspondence, from K. K. Yoon to S. Yukawa, "K Thermal Calculations," WG on Flaw Evaluations, Section XI, ASME Boiler and Pressure Vessel Code, July 5, 1993.

10. BAW-1543, Rev. 4, "Master Integrated Reactor Vessel Material Surveillance Program," B&W Owners Group, February 1993.

8. CERTIFICATION

This report is an accurate description of the low upper-shelf toughness fracture analysis of reactor vessels of the B&W Owners Group Reactor Vessel Working Group.

K K Yoon 12-13-93

K. K. Yoon, Advisory Engineer Date
Materials and Structural Analysis Unit

This report has been reviewed and is an accurate description of the low upper-shelf toughness fracture analysis of reactor vessels of Zion Units 1 and 2.

D E Killian 12-14-93

D. E. Killian, Principal Engineer Date
Materials and Structural Analysis Unit

Verification of independent review.

K E Moore 12-14-93

K. E. Moore, Manager Date
Materials and Structural Analysis Unit

This report is approved for release.

D L Howell 12/14/93

D. L. Howell, Project Manager Date
Reactor Vessel Services

APPENDIX A

Elastic-Plastic Fracture Mechanics Methodology

Typical reactore pressrue vessel steel exibits ductile tearing as the primary mode of fracture at the Charpy upper-shelf temperature range. J-integral based elastic-plastic fracture mechanics methods are used in this evaluation.

A.1. "J" Solution for Reference Flaw

For reactor vessel materials which can be modeled by deformation plasticity and whose stress-strain behavior can be represented by a power law strain-hardening equation, the $J_{applied}$ can be evaluated for the reference flaw[1] shown in Figure A-1 using the expression

$$J = J^E(a_{eff},P) + J^P(a,P,n) \qquad (A\text{-}1)$$

where J^E is the elastic contribution based on Irwin's effective crack depth, a_{eff}, and J^P is the deformation plasticity contribution from ref. 2. P is the applied pressure and n is the strain-hardening exponent. For the beltline area of the reactor vessel, the stress intensity factor for a semi-elliptical axial flaw on the inside of the vessel under pressure loading[3] is

$$K_I = \frac{PR_i}{t}\sqrt{\frac{\pi a}{Q}}\,F(a/\ell,a/t) \qquad (A\text{-}2)$$

where:

P = applied pressure

R_i = inside radius

t = thickness

$F = 0.97[M_1 + M_2(a/t)^2 + M_3(a/t)^4]f_s$

$M_1 = 1.13 - 0.18\,a/\ell$

$M_2 = -0.54 + 0.445/(0.1 + a/\ell)$

$M_3 = 0.5 - 1/(0.65 + 2a/\ell) + 14(1-2a/\ell)^{24}$

$$f_s = \left[\frac{R_o^2 + R_i^2}{R_o^2 - R_i^2} + 1 - 0.5\sqrt{\frac{a}{t}} \right] \frac{t}{R_i}$$

$$Q = 1 + 4.595(a/\ell)^{1.65}$$

ℓ = length of flaw

a = flaw depth

R_o = outside radius of vessel

$E' = E/(1 - \nu^2)$,

E = Young's modulus

ν = Poisson's ratio

then

$$J^E(a_e) = \frac{P^2 R_i^2}{t^2} \frac{\pi a_e}{Q} \frac{F^2}{E'} \qquad \text{(A-3)}$$

The effective crack size (a_e) is given by

$$a_e = a + \frac{1}{6\pi} \frac{(n-1)}{(n+1)} \frac{K_I^2}{\sigma_o^2[1+(P/P_L)^2]}$$

where: n = strain hardening exponent (Ramberg-Osgood)

σ_o = engineering yield stress

$$P_L = \frac{2}{\sqrt{3}} \sigma_o \frac{(t - a^*)}{(R_i + a^*)} \qquad \text{(A-4)}$$

The basic expression for the limit pressure, P_L, is for a continuous axial flaw. To obtain the limit pressure expression for a part-through wall flaw, the flaw size a is replaced by a* which is given as

$$a^* = \frac{a(1 - s)}{1 - (a/t)s} \qquad \text{(A-5)}$$

where: $s = (1 + \ell^2/2t^2)^{-0.5}$

The plastic part of J is given by the following expression

$$J^P = \alpha \frac{\sigma_o^2}{E} a(1 - a/t)h_1(P/P_L)^{n+1} \qquad \text{(A-6)}$$

where α and n are obtained from the Ramberg-Osgood stress-strain relation and h_1 is a dimensionless term which is a function of a/t, a/ℓ , n and t/R_i. This h_1 term is determined from the finite element results[4].

A2. "J" Solution for a Circumferential Flaw in a Cylinder

The acceptance criteria allow a reference flaw in the circumferential direction (Figure A-2) only in the case where there are only circumferential welds in the reactor vessel beltline region.

The K_I solution for a circumferential flaw shown in Fig. A-3 is from Kumar et al.[5]

$$K_I = \sigma \sqrt{\frac{\pi a}{Q}} F(a/\ell, a/t, R/t) \qquad \text{(A-7)}$$

where: σ = applied stress

$$\sigma = P \left[\frac{R_i^2}{R_o^2 - R_i^2} + 1 \right]$$

$$F = 1.026 + 0.27(a/t) + 0.40\,(a/t)^2 \qquad \text{(A-8)}$$

Eq. A-8 is a curve fit equation to the F factors tabulated in Ref. 34 as shown in Fig. 5.

Then,

$$J^E(a) = \frac{K_I^2}{E'} \qquad \text{(A-9)}$$

The effective crack size is given by

$$a_e = a + \frac{1}{6\pi}\frac{(n-1)}{(n+1)}\frac{K_I^2}{\sigma_o^2[1+(P/P_L)^2]} \qquad \text{(A-10)}$$

where: n = strain hardening exponent (Ramberg-Osgood)

σ_o = engineering yield stress

$$P_L = \sigma_o \Gamma \frac{(R_o^2 - R_i^2)}{R_i^2} \qquad \text{(A-11)}$$

$$\Gamma = [R_o^2 - R_c^2 + (1 - \gamma/\pi)(R_c^2 - R_i^2)]/(R_o^2 - R_i^2)$$

$$R_c = R_i + a_o + \Delta a$$

$$R_o = R_i + t$$

and

$\gamma = 3a/R_i$, flaw angle defined in Figure 3-5

The plastic part of J, J^P, for a constant depth and a finite length arc, part through flaw (Fig. A-5) solution is available from Ref. 6.

$$J^P = \alpha \frac{\sigma_o^2}{E} a \left(1 - \frac{a}{t}\right) h_1 \left(\frac{P}{P_L}\right)^{n+1}$$

where h_1 can be conservatively set at a constant value of 20.

Now total J is

$$J = J^E(a_e) + J^P(a)$$

A.3. J-Δa Analysis Method

For a given flaw size with appropriate crack extensions, applied J values may be calculated at a number of Δa values forming an applied J-Δa curve. Two of applied J-Δa curves, one for the accumulation pressure times safety factor of 1.15 plus the thermal gradient load case and another with the accumulation pressure times 1.25 and the thermal load are plotted against an appropriate lower bounding J-R curve as shown in Fig. A-7.

To check the first criterion, one must determine whether the applied J at crack size of a quarter of the vessel thickness plus 0.1 inch ($a = t/4 + 0.1$ inch) is less than the material J-R curve at $\Delta a = 0.1$ inch. And also the slope of the applied J curve should be less than the slope of the J-R curve at $\Delta a = 0.1$ inch point. By calculating several J applied values near 0.1 inch one can determine the slope of the applied J curve as indicated in Fig. A-6.

The second acceptance criterion is an instability check. To satisfy this criterion, an instability point load (or instability pressure) can be shown to be greater than the applied load with appropriate margin. Alternately, it is sufficient to demonstrate that the vessel under a combined load of 1.25 times of accumulation pressure, P_{acc}, and thermal gradient stress is "stable," as shown in Figure A-8.

By examining this plot one can estab sh that

$$J_{appl} = J_R \text{ at point A}$$

and

$$\frac{dJ}{da} < \frac{dJ_R}{da} \text{ at point A}$$

The flaw will not propagate beyond $\Delta a = \Delta a_A$ unless there is a further increase in the applied load. Therefore this structure with this flaw is stable under this prescribed loading condition.

A.4. Ramberg-Osgood Parameters

Ramberg-Osgood parameters are obtained by fitting the following equation to a true stress-strain curve.

$$\epsilon/\epsilon_o = \sigma/\sigma_o + \alpha\,(\sigma/\sigma_o)^n$$

Alternately, these parameters can be calculated by the following equations[7] using only yield and ultimate strength values of the material. This approach is used in this analysis.

$$\alpha = \frac{n\,(1.002 + \sigma_y/E)}{\sigma_y/E \times (1.002 + \sigma_y/E)^n}$$

$$\left[\frac{1/n}{\ell n\,(1.002 + \sigma_u/E)}\right]^{1/n} - \frac{\sigma_u\, e^{1/n}}{\sigma_y\,(1.002 + \sigma_y/E)} = 0$$

where

σ_y = yield stress

σ_u = ultimate strength

E = Young's modulus

Figure A-1. Geometry of Reactor Vessel Beltline With ASME Appendix G Postulated Flaw

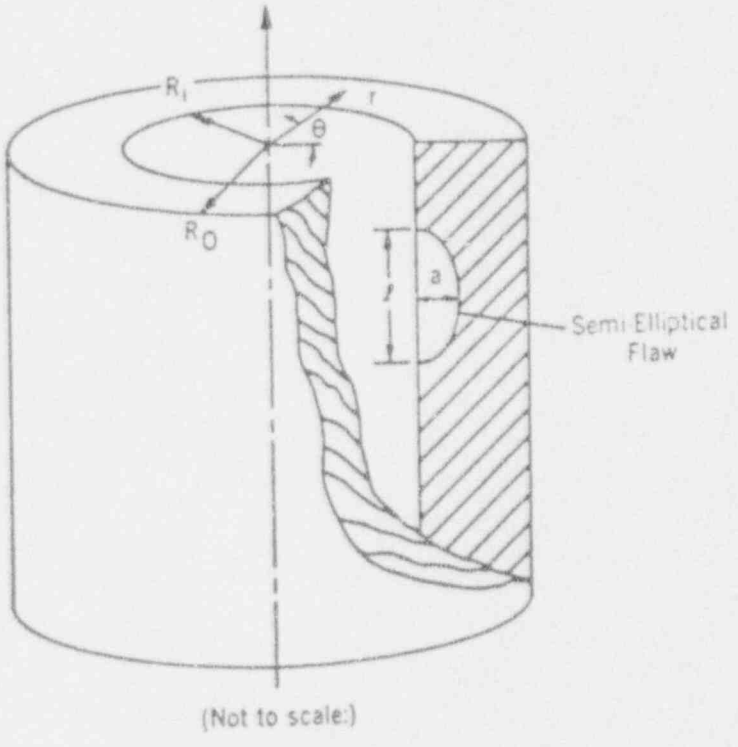

Figure A-2. Postulated Circumferential Flaw

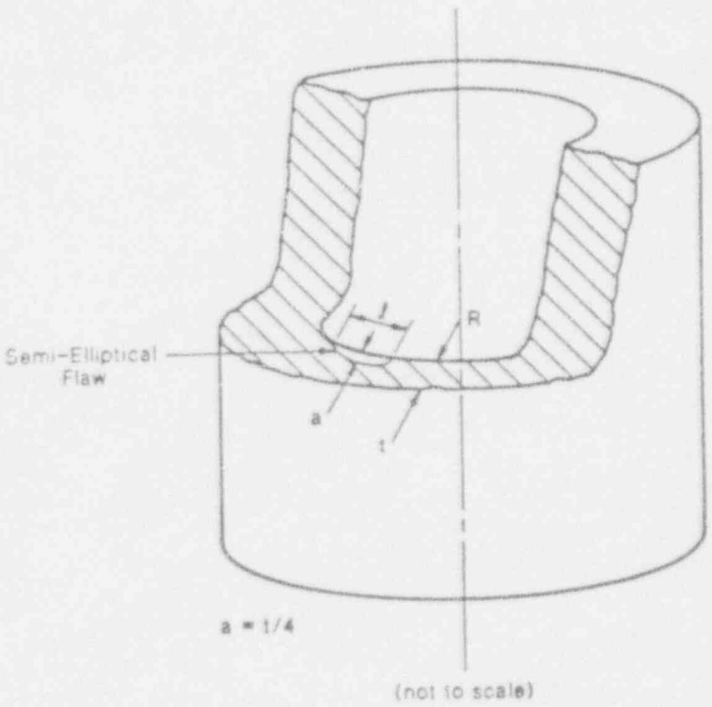

Figure A-3. Schematic of a Part-Through, Circumferential Surface Flaw in a Cylinder - Elliptical Flaw

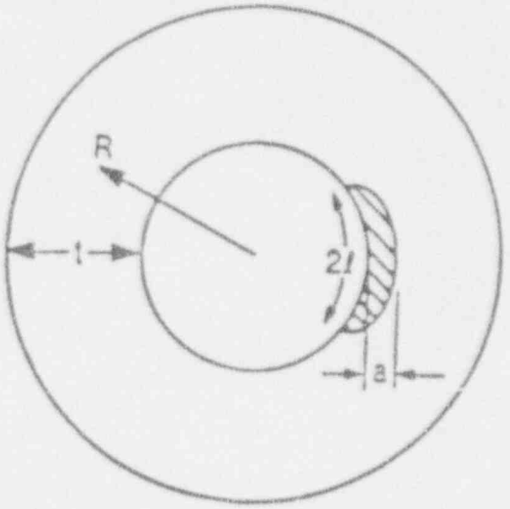

Figure A-4. Schematic of a Part-Through, Circumferential Surface Flaw in a Cylinder - Constant Depth Flaw

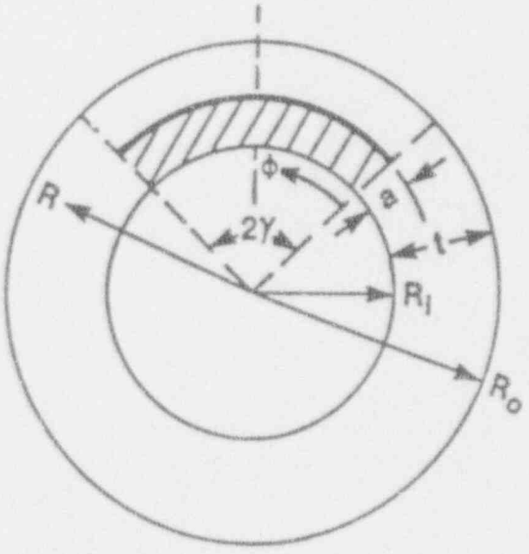

Figure A-5. F Factors and Curve Fit Equation

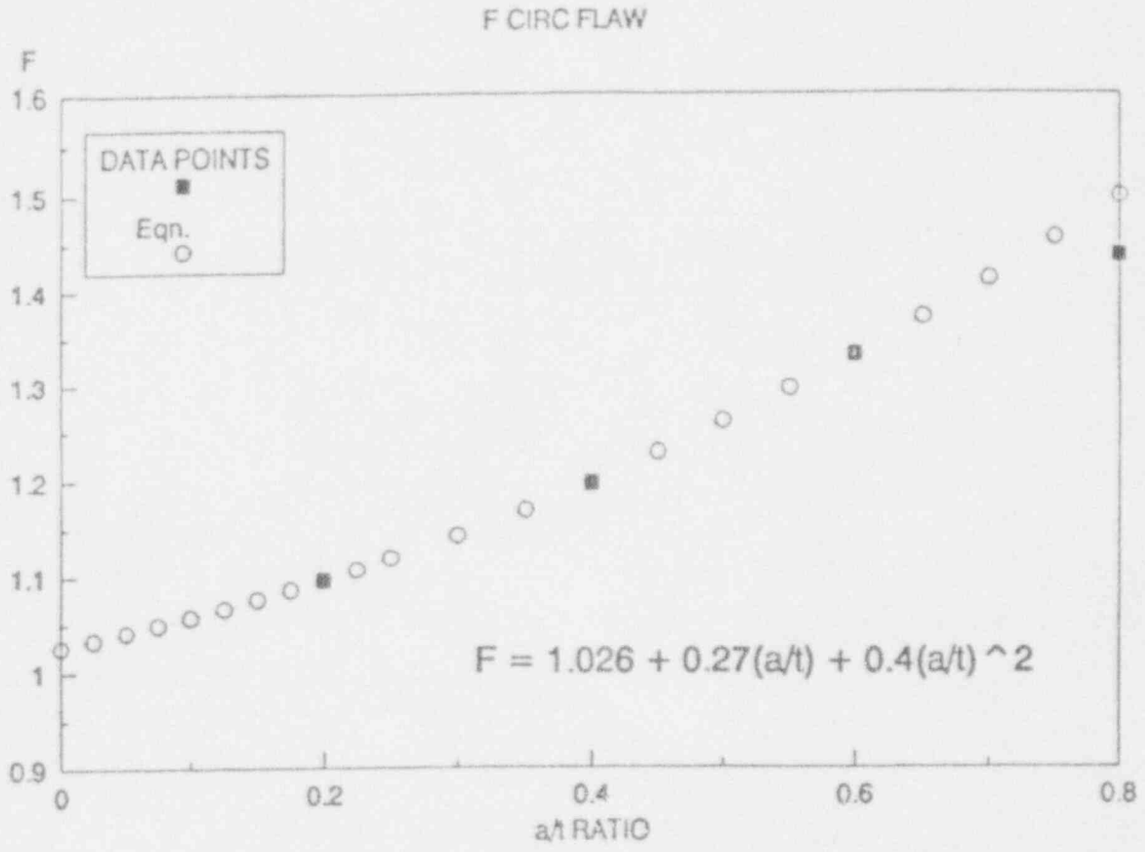

Figure A-6. Deformation Plasticity Failure Assessment Diagram

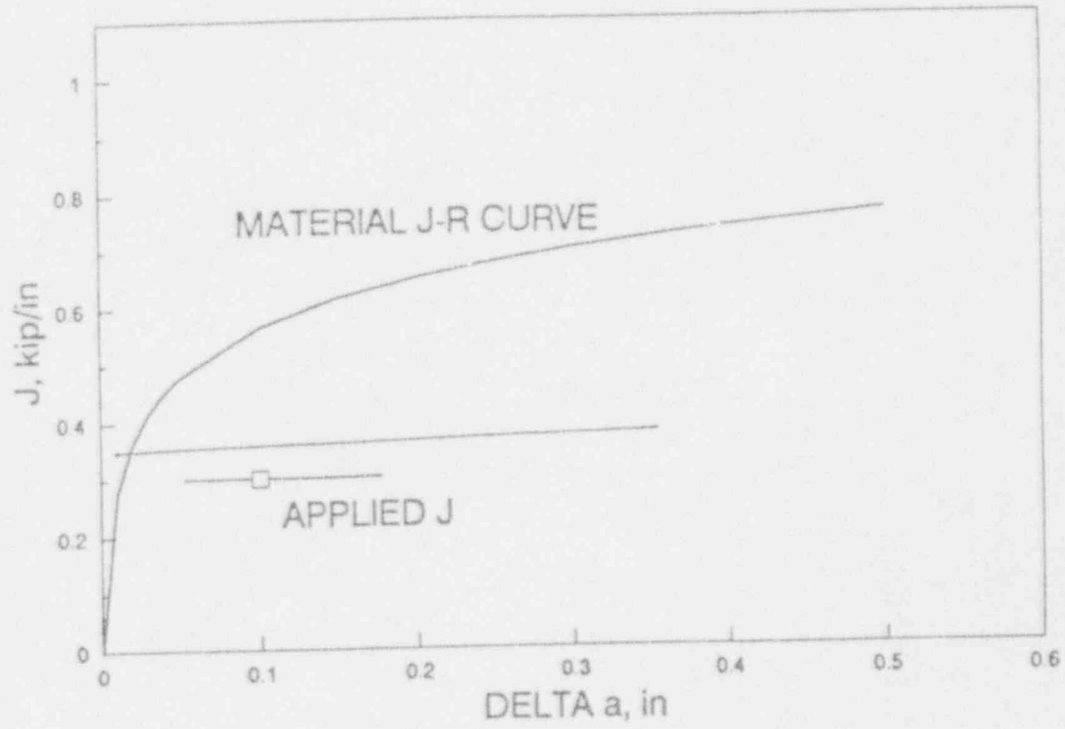

Figure A-7. J-Δ a Analysis

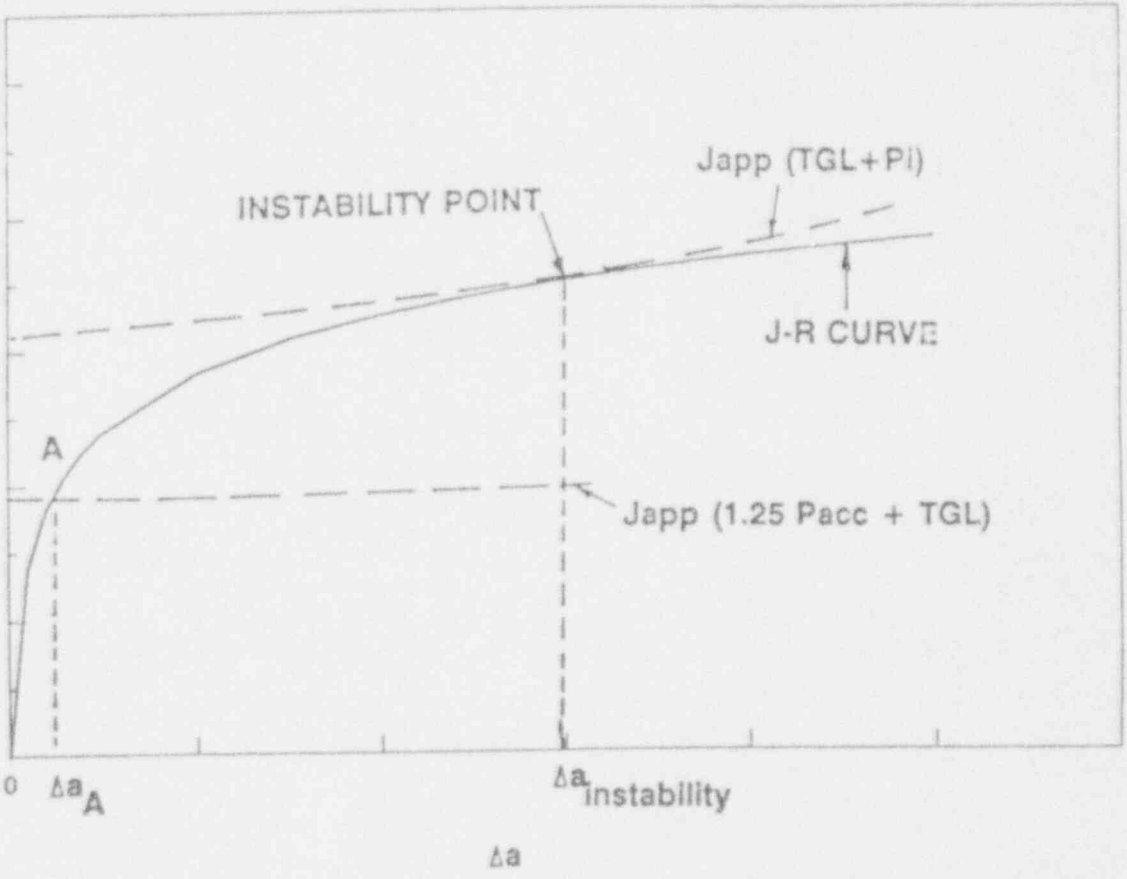

PI - Instability pressure

TGL - thermal gradient load

APPENDIX B

Material Property Characterization

B.1. Fracture Toughness Model Development Methods

The objective of the fracture toughness model development is, in the absence of a physical model describing the irradiated J-resistance (J-R) behavior of the Linde 80 material, to empirically extract all variables affecting the behavior of J-R properties of Mn-Mo-Ni/Linde 80 welds and the inter-relationship among these key variables. The resulting mathematical model facilitates two very important necessary functions. The model enables any interpolation or extrapolation of the variables selected in the model and also provides a means to define a lower bounding limit to satisfy the regulatory requirement of the material J-R curve.

Recent developments in pattern recognition techniques provided a new method to obtain mathematical models of materials data behavior. In 1989, it was demonstrated through a pilot program under the NRC's sponsorship[8] that J-R data can be analyzed by this approach. Additional work was performed to model the HSST J-R data[9]; the software that was used in those programs were applied to the current B&W Owners Group data analysis in this report.

The primary data analysis methods are the ACE and SURFIT computer programs developed by Modeling and Computing Services. Data analysis and model construction using these two programs are discussed below.

B.1.1. Key Variables and Model Form

Advanced methods of data analysis have recently been developed to allow simultaneous consideration of the effects of many variables and to allow the data and/or physical considerations to establish the best model form.

In usual statistical approaches, modeling forms (usually linear) are assumed and then compared to the data. The advanced methods use the data directly to show the analyst the form of model to use.

The ACE computer code identifies key variables and the optimal form of function to use for multivariable surface-fitting, going directly from the data without restrictive assumptions about

the form of the model. ACE identifies the numerically defined transformations $\theta(y)$ and $\phi_j(x_j)$ such that

$$\theta(y) = \sum_{j=1}^{n} \phi_j(x_j) \tag{B-1}$$

The transformations are not chosen in advance, instead they are the unknowns that are calculated by ACE and are displayed graphically. The form specified by Eq. B-1 is very general, capable of representing any function of a sum of arbitrary functions, products of arbitrary functions.

ACE does not actually use mathematical forms for the transformations; it numerically smooths the raw data. ACE alternately estimates pointwise values of $\theta(y)$ given all $\phi_j(x_j)$, then each $\phi_j(x_j)$ given $\theta(y)$, and iteratively refines these estimates until the error in satisfying Eq. B-1 is minimized in a least squares sense. The mathematical algorithm and an elegant proof of convergence and optimality were presented in Ref. 10. The method can be proven to converge to unique, optimal transformations under certain conditions, and it works well in practice on multivariable nonlinear problems.

ACE requires as input the raw data in a matrix format

$$\begin{array}{ll} y_1 & x_{11}\ x_{12}\ x_{13}\ x_{14}\ \cdots\ x_{1n} \\ y_2 & x_{21}\ x_{22}\ x_{23}\ x_{24}\ \cdots\ x_{2n} \\ \vdots & \\ y_m & x_{m1}\ x_{m2}\ x_{m3}\ x_{m4}\ \cdots\ x_{mn} \end{array} \tag{B-2}$$

where the independent variables x_{ij} can be either continuous or categorical. Typical categorical variables might be material form, i.e. plate or forging or weld, or different laboratories or investigators when correlating any type of data from multiple sources. ACE is very useful for identifying laboratories or investigators that produce outlier results.

The output from ACE is in graphical form, including plots of each transformed variable. The plots are presented in standard deviation coordinates so that it is easy to identify the variables that account for most of the apparent scatter in response values. This is important since a variable that accounts for three standard deviations of "scatter" in response values is a more important variable for modeling than one that only accounts for one standard deviation. The plots also indicate by their shape the mathematical forms that should be used for modeling the data. After viewing the plot, the analyst can choose a functional form and confirm the choice by introducing transformed variables $\theta(y)$ and $\phi_j(x_j)$ in place of the original variables y, x_j in Eq. 4-2 and reapplying ACE. Theoretically-based mechanistic models can be introduced in the same way, if desired. If the appropriate functional form is chosen, the ACE plots will be nearly linear on the second try. Note that the data establish the form of the transformations; the analyst only checks potential mathematical forms after looking at the results. This is a fundamental advance over previous ways of doing modeling and data analysis.

B.1.2. Model Calibration

Once the important variables have been identified and the shapes of the functional relationships for each term have been determined, the remaining task is to develop a working model and estimate its parameters. The data are then normalized to a common set of conditions using the model. The normalizing step is essential for correlating multivariable data since only when the data are normalized by a fitted model can the trends in each variable be clearly seen.

SURFIT is a nonlinear least squares surface fitting code that allows complete freedom in specification of the fitting functions. Whatever functions that appear useful, based on ACE analysis and theoretical considerations, can be conveniently introduced to SURFIT. Constraints and weighting can be imposed to give greater emphasis to higher quality data or known asymptotic values. The analyst can also control the form of the residuals, allowing fits that minimize absolute residuals, log residuals, relative error, and residuals perpendicular to the model. The input to SURFIT is the same form as Eq. B-2, plus a user-defined fitting function.

Minimization of the sum of squares of the residuals is performed numerically, using a modification of the Powell nonlinear least squares algorithm[11].

Use of ACE and SURFIT is an iterative process, since the results of ACE provide insight to SURFIT model forms and vice versa. The first successful application of this approach to J-R model was made for the NRC and followed by an expanded program in 1990[9].

B.2. Data Analysis

B.2.1. B&W Owners Group Data Base Description

In the elastic-plastic fracture mechanics analysis as proposed in this report, toughness is in terms of the J-resistance (J-R) curve and strength properties are in the form of Ramberg-Osgood parameters which need a true stress-strain curve. The B&W Owners Group data base has both J-R and stress-strain data. The Integrated Reactor Vessel Surveillance Program (IRVSP) conducted over the last 15 years has accumulated a large body of J-R data including irradiated and unirradiated specimen test results. Table B-1 shows the extent of the B&W Owners Group data base for J-R curves and additional J-R data are available from the NRC HSST program.

Since this report deals specifically with the low upper-shelf issue, these J data were further screened to obtain those J-R data relevant to the upper-shelf temperature range. Data below 390 F was excluded based on the following reasoning. The K_{Ic} curve found in Section XI of the ASME Boiler and Pressure Vessel Code (Fig. B-1) shows that K_{Ic} reaches 200 ksi $\sqrt{in.}$, the upper-shelf toughness, when the T minus RT_{NDT} value is above approximately 105 F. Assuming that for the greatest irradiation-damaged weld metal RT_{NDT} is the same as the PTS screening criteria[12], 270 F, the choice of 390 deg F assures that all J-R data above this temperature is at the upper-shelf level.

B.2.2. J Control Limit

ASTM Standard E1152-87[13] allows ten percent of the initial ligament to be the validity limit for crack extension in compact specimen testing. However, many researchers found that ductile tearing data behave nicely far beyond the ASTM recommended limit. In particular, Mn-Mo-Ni/Linde 80 J-R data show valid data range from 35 to 50 percent of the initial ligament. Joyce[14] proposed a method to define an engineering J control limit based on a relationship between plastic displacement and crack extension. This method suggests that the point where the deviation from the linear slope is 5 percent may be taken as the J control limit. A sample plot in Fig. B-2 shows that the deviation from the linearity starts at a crack extension equivalent to 36 and 44 percent of the initial ligament. For this evaluation, a conservative validity limit was selected: 35 percent of the initial ligament.

B.2.3. Data Assembly

Prior to running pattern recognition, the Mn-Mo-Ni/Linde 80 weld J-R data were assembled. J-Δa points beyond the J control limit were excluded and those data points with test temperature less than 390 F were also excluded to assure a data base for the upper-shelf temperature range only. In addition, data points with Δa less than 0.01 were eliminated since J values at small Δa values usually exhibit larger scatter.

B.2.4. Candidate Variables for J-R Model

The following variables were selected for consideration:

Fluence - Fluence strongly affects material degradation and is clearly a candidate variable.

Test Temperature - It was observed as test temperature increases, the J values decrease for Mn-Mo-Ni/Linde 80 weld metal.

Chemical Composition - The effect of chemical composition on irradiation damage is well known; the nine elements are therefore included in the selection as shown in Tables B-2 and B-3.

Specimen Size - As specimen size has been shown to be a variable in J_d sets, therefore, net specimen thickness was selected as a candidate variable.

Data Group - To determine whether "power reactor" and "test reactor" irradiations have distinctly different patterns, data group name was selected as a categorical variable.

Yield and Ultimate Strengths - To investigate the impact of mechanical strength properties to J value, these two are included as candidate variables.

Uniform Elongation - This property is also selected as a candidate variable.

Charpy Energy - This is selected to show whether Charpy energy value can represent the irradiation damage in place of the fluence.

B.2.5. Pattern Recognition and Model Form

The data plots in Figures B-3 and B-4 show all the raw J-Δa points assembled for pattern recognition analysis. To determine the pattern of the data behavior, the ACE program was run using trial transformations of the Y variable and the seventeen candidate variables. Based on earlier work performed by the B&W Owners Group, it was learned that the following J equation best describes J-R curves for Mn-Mo-Ni/Linde 80 weld metals.

$$J = C1\ (\Delta a)^{C2} \exp(C3\ \Delta a^{C4}) \qquad \text{(B-3)}$$

Equation B-3 is a power law expression with a modifier exponential function that better fits the small Δa part of the J-R curve. The power law behavior of J-R data points can be seen in Figures B-3 through B-4.

Figures B-5 and B-6 are the transformation analysis output from ACE showing that the natural logarithm of C1 from the J equation strongly influences the data set. Relying on the insights gained by early NRC data analysis[8] and a series of power law fit model development work by the B&W Owners Group, application of ACE showed that four variables had major effects on the data set, as shown in Figures B-7 through B-12. These variables are fluence, copper content, temperature, and specimen size. The remaining variables from the initial selection of seventeen variables are insignificant. Through numerous trials to find the optimum functional relationships among these variables, it was learned that a product of copper content and fluence is more significant as a key variable than when considered separately. This product was further refined by raising the fluence to the power "a" thus:

$$Cu\ (\phi t)^a$$

where Cu is the copper content in weight percent, ϕt is fluence in units of 10^{18} n/cm^2, and a is a number less than unity.

The current low upper-shelf toughness issue regulation is based on Charpy upper-shelf values. Charpy absorbed energy values are taken as an indication of fracture toughness. In this data analysis, the Charpy upper-shelf energy (CvUSE) is used as an alternative parameter to account for irradiation damage to fracture toughness; this assumes that irradiation effects are reflected in the Charpy test results of irradiated specimens. Use of CvUSE as a fracture toughness degradation indicator was partly based on the observation that the initial plant surveillance programs had mostly Charpy specimens and very few, if any, CT specimens. There is no definite mechanistic linkage between CvUSE and J-R curves to date. In the present data analysis effort, CvUSE is selected to be an alternate variable in place of the $Cu(\phi t)^a$ term; both terms were used for model development.

The current model form of the J-R equation is obtained as follows:

From $$J = C1\ (\Delta a)^{C2} \exp(C3\ \Delta a^{C4}) \qquad \text{(B-3)}$$

Take natural logarithms:

$$\ell n\ J = \ell n\ C1 + C2\ \ell n(\Delta a) + C3\ (\Delta a)^{C4}$$

A series of combinations of the proposed model were tried. When a form of the model was derived through repeated and improved combinations and transformations, the following final form was obtained:

$$\ell n\ C1 = a1 + a2\ \ Cu(\phi t)^{a7} + a3\ T + a4\ \ell n\ B_N \qquad \text{(B-4)}$$

$$C2 = d1 + d2\ \ell n\ C1 + d3\ \ell n\ B_N \qquad \text{(B-5)}$$

$$C3 = d4 + d5\ \ell n\ C1 + d6\ \ell n\ B_N \qquad \text{(B-6)}$$

where T is temperature in F, B_N is net specimen thickness in inches and Cv is the Charpy upper-shelf energy in ft-lb. It is noteworthy that J_M takes d3 and d6 as zeroes, indicating that specimen size dependency is not applicable.

B.2.6 Determination of Optimal Parameters

SURFIT was applied to the above model (Paragraph B.2.5), first against the combined data set of HSST and B&W Owners Group data and second only against the B&W Owners Group set to determine optimal sets of constants in the equation, C1 through C4, by means of constants a's and d's. By applying these constants in Equations B-4 through B-6, a specific J-R curve can be generated for a particular application. The results are tabulated in Tables B-4 and B-5.

B.2.7. Model Verification

To verify how the above multivariable equation fits all the test data used to develop this equation, a series of verification plots are made on a standard condition. There are more than 1300 data points in the B&W Owners Group data set and more than 3300 points in the combined B&W Owners and HSST data set. Any single data point from this set represents a unique condition, i.e. specific fluence, temperature, specimen thickness, and copper content. Since the model equation represents functional relationships among these variables, this data point can be converted to a standard condition - normalized condition selected based on typical values of all variables. The standard condition selected for the normalization is

fluence, $\phi t = 8.0 \times 10^{18}$ n/cm^2

flaw extension, $\Delta a = 0.1$ in.

temperature, $T = 480$ deg F

specimen thickness, $B_N = 0.8$ in.

copper content, Cu = 0.30 wt%

Normalization is made based on the following conversion equation,

$$J_{i\ \text{std. cond.}} = J_{i\ \text{test data}} \left[J_{\text{calc @ std cond.}} / J_{\text{calc @ith cond}} \right]$$

When all the data points are converted to the normalized condition, these points will form a master J-R curve for the standard condition if the model is reasonable. Such normalization has been performed and the results are shown in Figures B-13 and B-14. These are plots of an overall normalized J versus Δa curves. The overall fit is very good considering the range of variables involved in the entire data set, providing a master J-R curve of Mn-Mo-Ni/Linde 80 weld metal for the standard condition.

Further, to determine the effect of individual variables on the data set, normalized variables were shown against the standard deviation of the data set. Figures B-15 through B-18 show these effects for the B&W Owners Group data set. Similar trends are true for modified J, J_M.

The final J-R model, equation B-3 with all the necessary parameters, are defined by a set of equations, B-4 through B-6. The constants a's and d's needed to determine the parameters are tabulated in Tables B-4 and B-5.

B.3. Power and Test Reactor Toughness Data

The B&W Owners Group Integrated Reactor Vessel Surveillance Program power reactor irradiations were conducted in Crystal River Unit 3 and Davis Besse Unit 1. Both of these reactors have similar neutron spectrum characteristics and, therefore, the data can be used interchangeably. A nominal fast neutron flux in these commercial power reactors is 7.4×10^{10} n/cm^2/sec. In contrast, the flux in the test reactor where the HSST specimens were irradiated has a nominal flux of 1.5×10^{12} n/cm^2/sec. Since there is no well established mechanistic model for flux effects on the long term irradiation damage in metal structures, only an empirical observation is possible at this point. One such observation can be made through this type of modeling effort. As a categorical variable there are some differences between the power reactor irradiated specimen data and the HSST irradiated specimen data. However, the magnitude is insignificant in terms of total standard deviation of the combined data set. Further, difference may occur from the fact that the HSST program has more larger-size specimens and irradiated to fluences above 8.5×10^{18} n/cm^2. The power reactor specimens were irradiated to fluences

of 8.5×10^{18} n/cm^2. Therefore, it is concluded that there is no significant difference in two data sets for this class of weld metal irradiated J-R test data.

B.4. J-R Model Prediction Trends

A mathematical model for Linde 80 weld metals is now available and in this section a number of trends exhibited by this model will be studied. Among the key contributing variables, effects of the fluence term can be seen in Figure B-19, where J at $\Delta a = 0.1$ inch is plotted against fluence with four levels of copper content and temperature and specimen size held constant. It is noteworthy that there is an initial drop of J from the unirradiated condition to the first level of fluence calculated, then almost linearly decreasing Js with increasing fluence can be observed.

Figure B-20 shows a plot of J at 0.1-inch crack extension versus test temperature with varying fluence level and a fixed copper content and a fixed B_N. In Figure B-21, J at 0.1 inch crack extension is plotted against specimen thickness at various copper content at a fixed value of fluence. Compared to the normalized data plots in the previous sections, these trends support the data behavior as expected.

Table B-1. Summary of B&W Owners Group J-R Data Base

Number of Compact Specimens	230
Test Temperature Range	70 ~ 500 F
Number of Irradiated Specimens	110
Range of Fluence on Irradiated Specimens	1.17 ~ 8.45 x 10^{18} n/cm^2
Specimens Test at Temperature Greater than 390 F	
Irradiated Specimens	58
Unirradiated Specimens	48

Table B-2. Chemical Composition of Weld Metals in Data Base Used to Develop Correlation Models

		Chemical Composition, wt%								
Item	Weld ID	C	Mn	P	S	Si	Cr	Ni	Mo	Cu
1	WF-193A	0.09	1.49	0.016	0.016	0.51	0.06	0.59	0.39	0.28
2	WF-182-1	0.09	1.69	0.014	0.013	0.41	0.15	0.63	0.40	0.21
3	SA-1263	0.09	1.47	0.019	0.024	0.49	0.13	0.57	0.39	0.22
4	SA-1036	0.08	1.41	0.012	0.016	0.59	0.09	0.56	0.36	0.23
5	SA-1101	0.08	1.56	0.019	0.008	0.59	0.16	0.54	0.38	0.21
6	SA-1094	0.10	1.44	0.014	0.011	0.50	0.14	0.60	0.36	0.30
7	SA-1526	0.09	1.53	0.013	0.017	0.53	0.08	0.68	0.42	0.35
8	WF-233	0.10	1.45	0.021	0.015	0.42	0.08	0.68	0.44	0.27
9	WF-25	0.09	1.58	0.015	0.016	0.54	0.09	0.67	0.42	0.35
10	WF-67	0.08	1.55	0.021	0.016	0.58	0.10	0.60	0.40	0.22
11	SA-1585	0.08	1.45	0.016	0.016	0.51	0.09	0.59	0.38	0.21
12	WF-70	0.09	1.63	0.018	0.009	0.54	0.11	0.59	0.40	0.42
13	WF-112	0.08	1.47	0.016	0.015	0.54	0.07	0.59	0.40	0.32
14	SA-1135	0.08	1.45	0.011	0.013	0.49	0.08	0.59	0.38	0.27
15	WF-209-1	0.11	1.55	0.022	0.010	0.65	0.09	0.58	0.39	0.36
16	WF-292	0.13	1.47	0.009	0.011	0.61	0.09	0.62	0.45	0.03
17	SA-1118	0.08	1.29	0.013	0.014	0.61	0.09	0.57	0.39	0.32

Table B-3. Chemical Composition of HSST Submerged-Arc Welds

Weld	Average Composition, wt%[a]								
	C	Mn	P	S	Si	Cr	Ni	Mo	Cu
61W	0.09 0.07 0.10	1.48 1.45 1.52	0.020 0.018 0.021	0.014 0.014 0.015	0.57 0.55 0.58	0.16 0.16 0.17	0.63 0.62 0.64	0.37 0.36 0.38	0.28 0.26 0.31
62W	0.083 0.078 0.088	1.51 1.41 1.61	0.016 0.013 0.020	0.007 0.007 0.008	0.59 0.55 0.63	0.120 0.067 0.173	0.537 0.490 0.585	0.377 0.365 0.390	0.210 0.160 0.260
63W	0.098 0.088 0.109	1.65 1.62 1.67	0.016 0.015 0.017	0.011 0.010 0.013	0.630 0.580 0.675	0.095 0.073 0.118	0.685 0.663 0.707	0.427 0.415 0.440	0.299 0.272 0.326
64W	0.085 0.070 0.100	1.59 1.54 1.64	0.014 0.012 0.017	0.015 0.014 0.016	0.520 0.445 0.600	0.092 0.074 0.110	0.660 0.600 0.720	0.420 0.410 0.430	0.350 0.310 0.390
65W	0.080 0.070 0.090	1.45 1.42 1.49	0.015 0.014 0.017	0.015 0.013 0.017	0.480 0.450 0.610	0.088 0.076 0.100	0.597 0.585 0.610	0.385 0.370 0.400	0.215 0.180 0.250
66W	0.092 0.075 0.110	1.63 1.59 1.67	0.018 0.017 0.020	0.009 0.009 0.010	0.540 0.480 0.600	0.105 0.090 0.120	0.595 0.580 0.610	0.400 0.380 0.420	0.420 0.350 0.490
67W	0.082 0.070 0.095	1.44 1.40 1.48	0.011 0.010 0.013	0.012 0.012 0.013	0.500 0.410 0.590	0.089 0.067 0.110	0.590 0.580 0.600	0.390 0.370 0.410	0.265 0.220 0.310

[a]Top entry is the average value, while numbers shown below each entry indicate the range of composition measurements.

Table B-4. Parameters in J_D Model

	Model 4A[1] B&W JD	Model 4B[2] B&W JD
a1 a2 a3 a4 a7		
d1 d2 d3 d4 d5 d6		
# of points SIG ()^2 in ln(J) Se in ln(J) Se in log(J)		
Ratio -1 Se -2 Se -3 Se		

[1]CV Based Model

[2]Cu*Fluence^N Based Model

Table B-5. Parameters in J_M Model

	Model 4A[1] B&W JM	Model 4B[2] B&W JM
a1 a2 a3 a4 a7		
d1 d2 d3 d4 d5 d6		
# of points SIG ()^2 in ln(J) Se in ln(J) Se in log(J)		
Ratio -1 Se -2 Se -3 Se		

[1]CV Based Model

[2]Cu*Fluence^N Based Model

Figure B-1. K_{IC} Curve

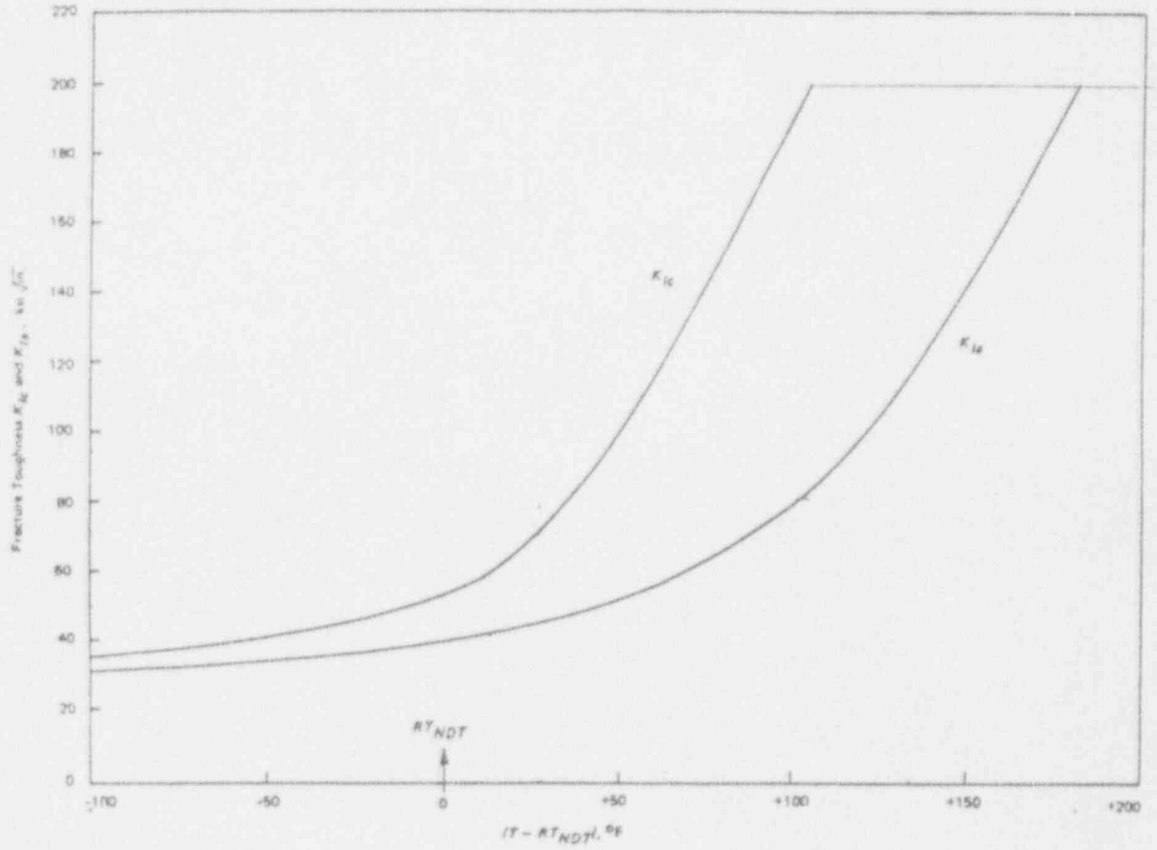

Figure B-2. J Control Limit Assessment

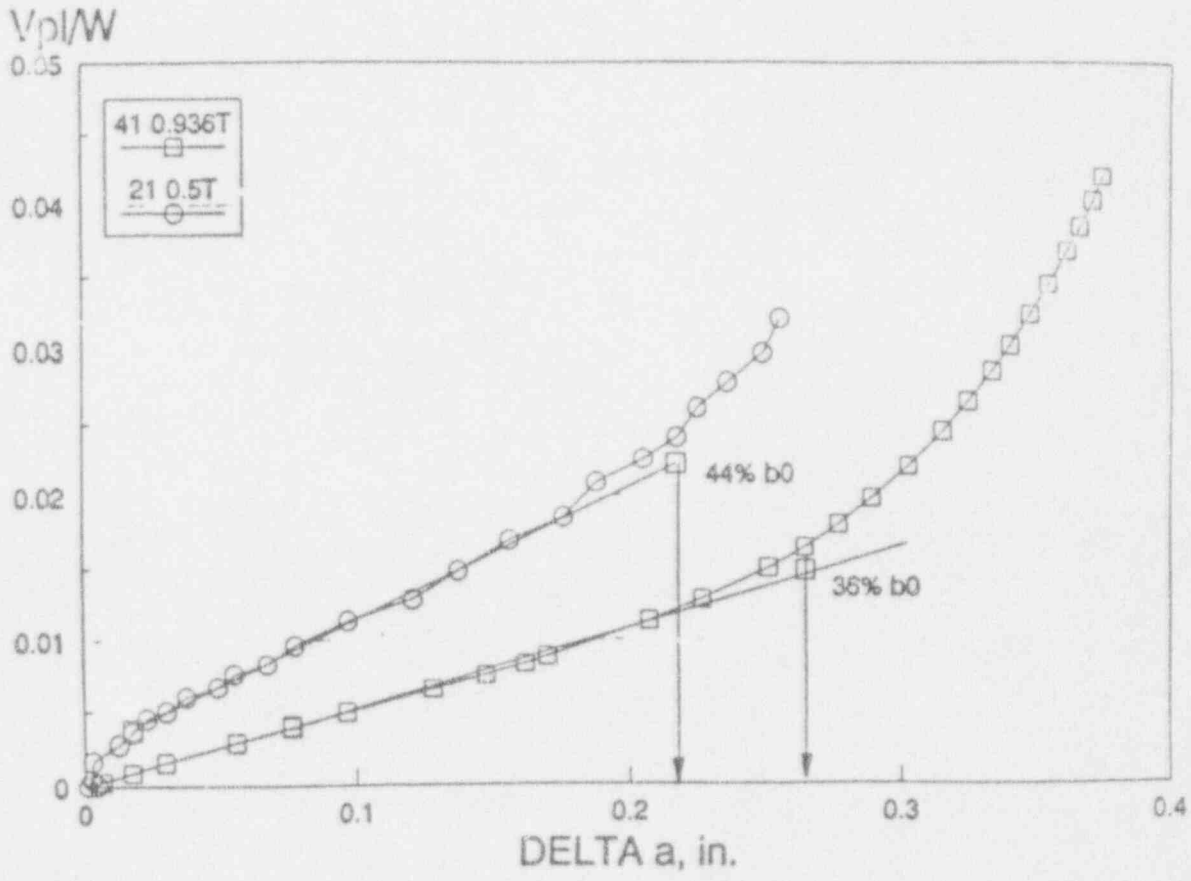

Figure B-3. B&WOG Data on Log-Log Scale - J_D-Δa

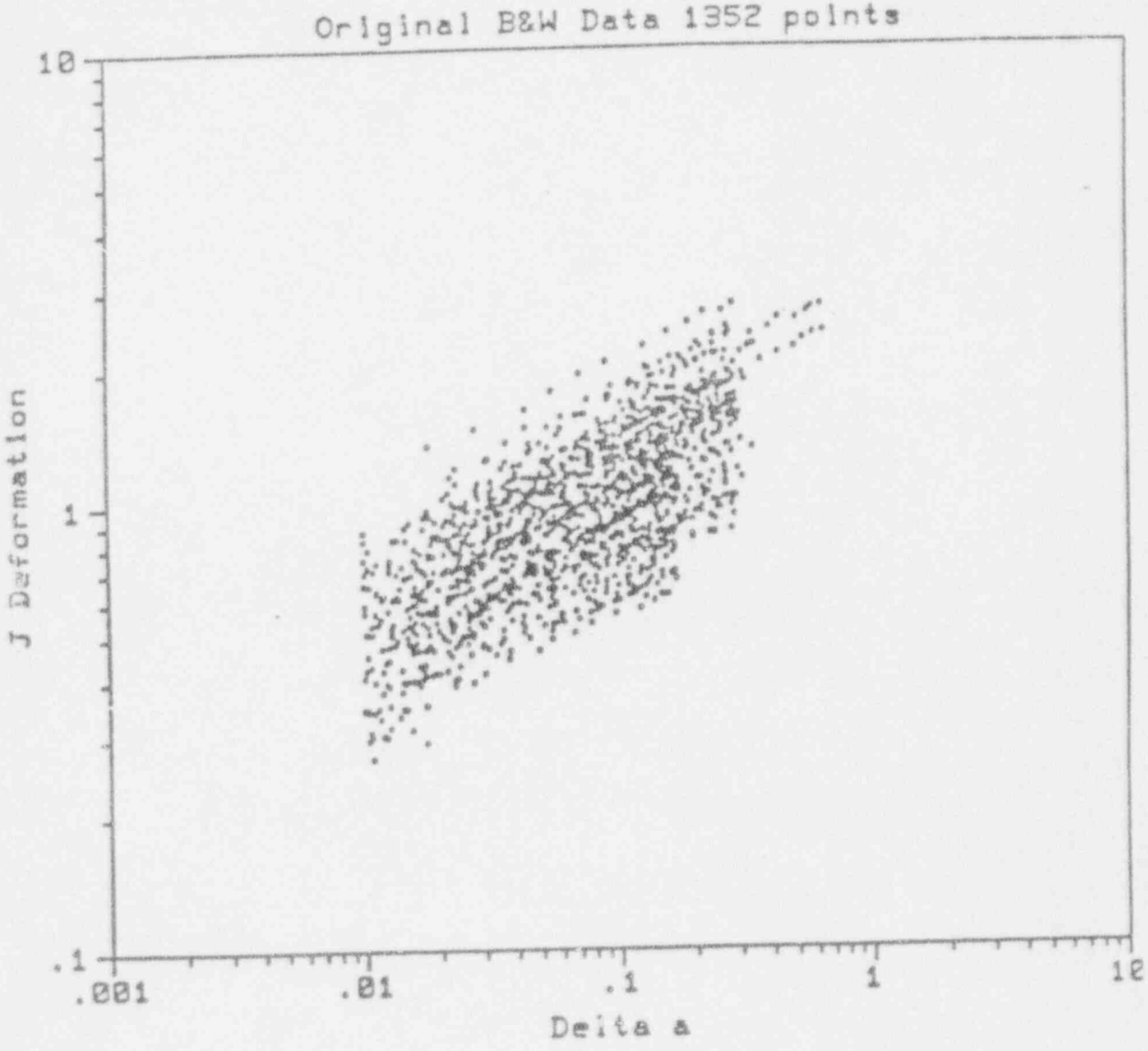

Figure B-4. B&WOG Data on Log-Log Scale - J_M-Δa

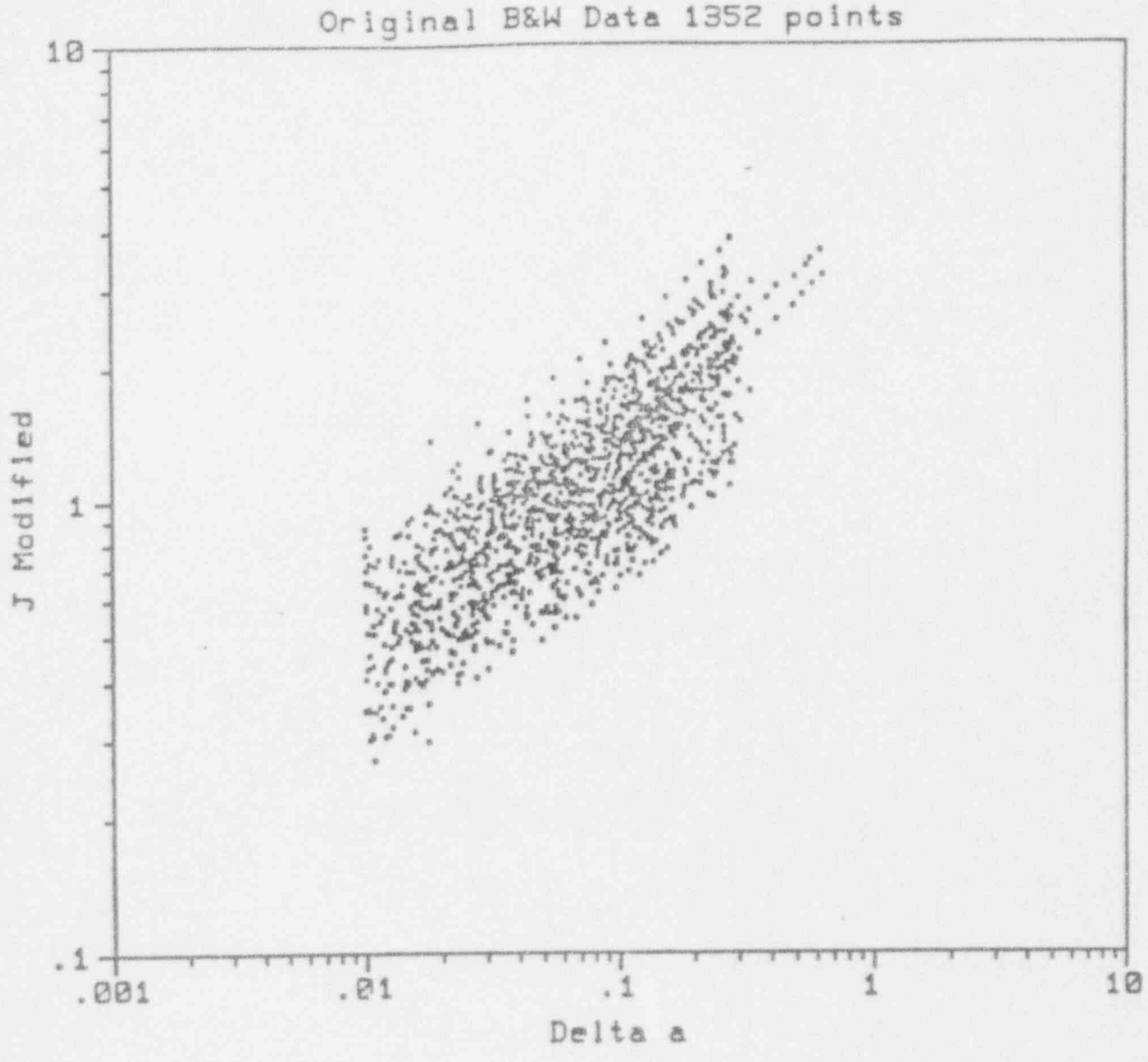

Figure B-5. Transformation Analysis Plot (TAP) for ln C_1 - J_D

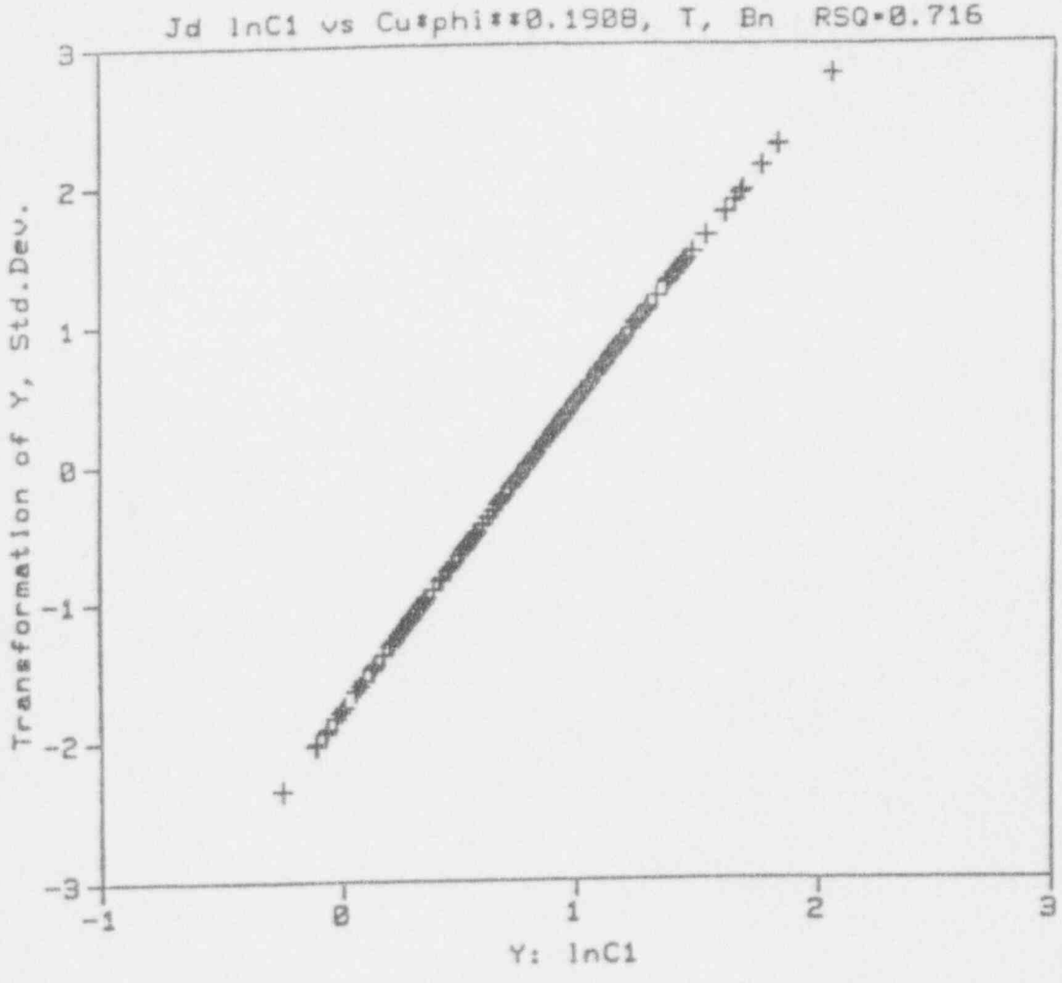

Figure B-6. Transformation Analysis Plot (TAP) for ln C_1 - J_M

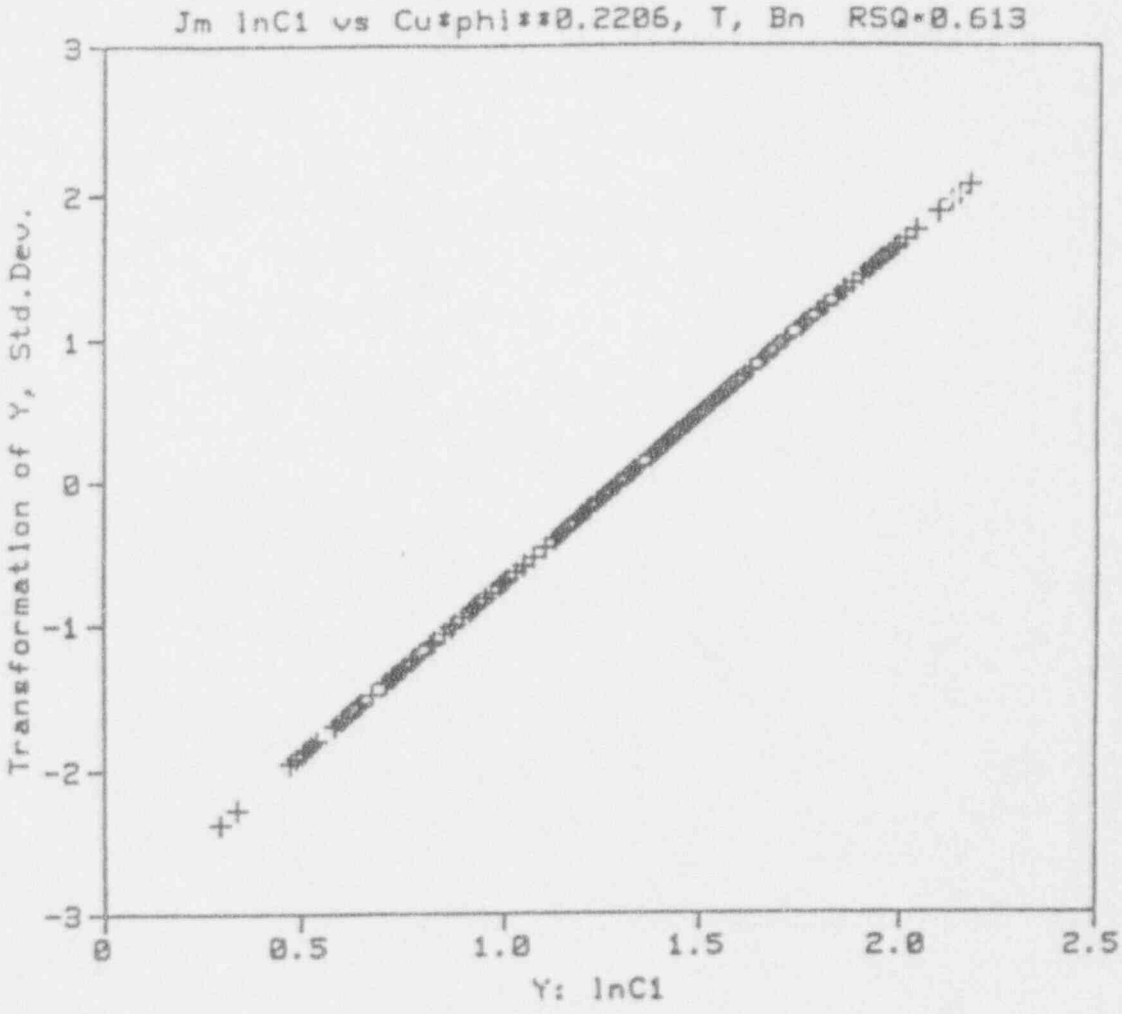

Figure B-7. TAP for Cu x Fluence$^{0.1908}$ on J_D

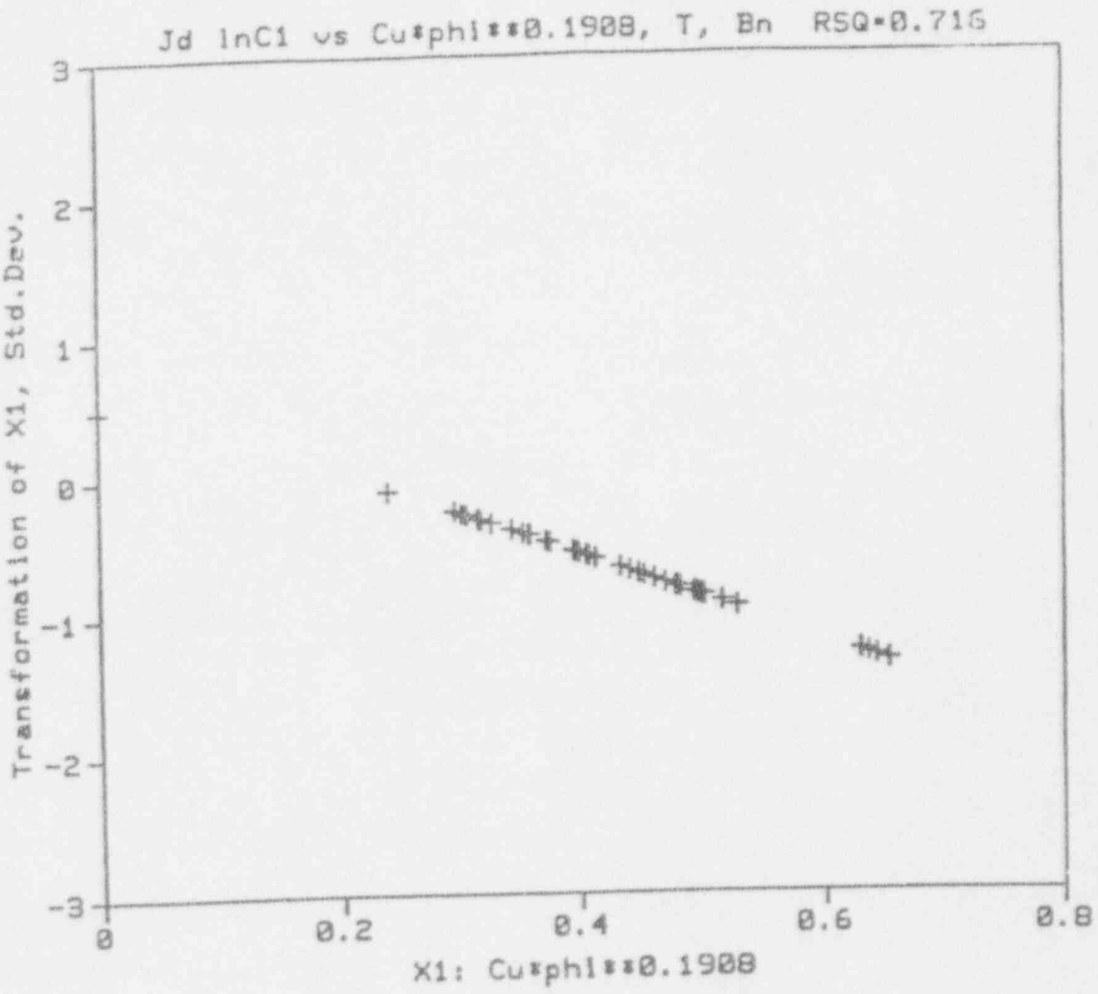

Figure B-8. TAP for Cu x Fluence$^{0.1908}$ on J_M

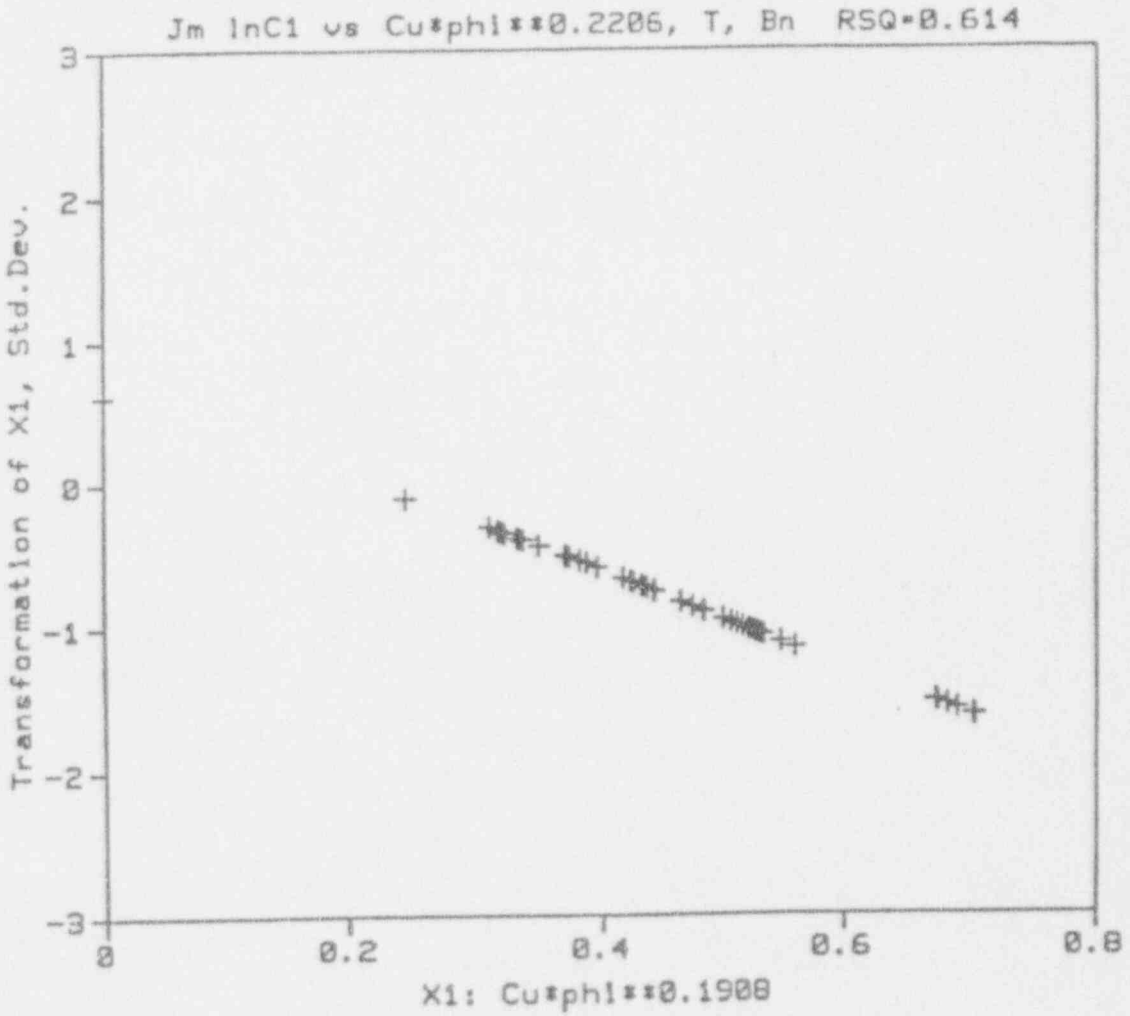

Figure B-9. TAP for Temperature on J_D

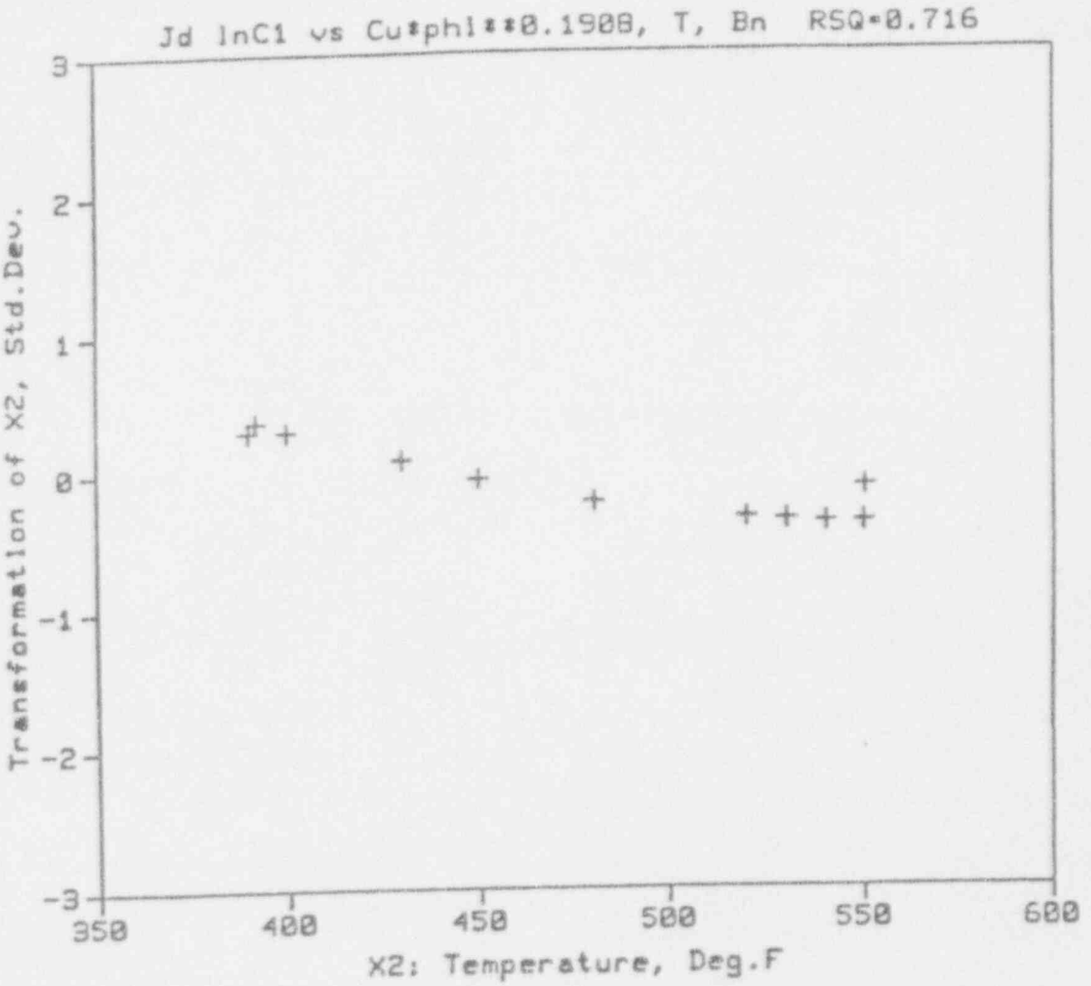

Figure B-10. TAP for Temperature on J_M

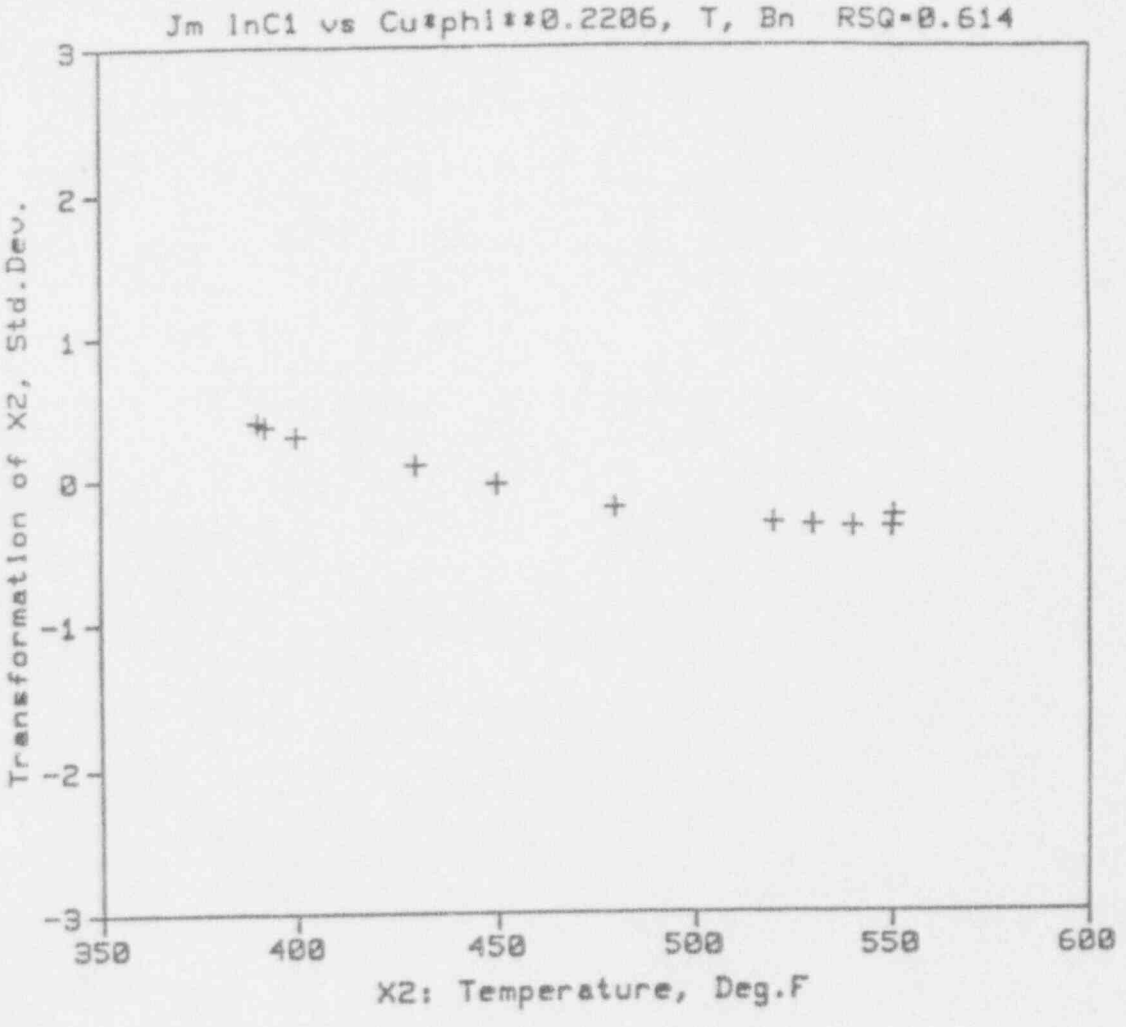

Figure B-11. TAP for Net Thickness on J_D

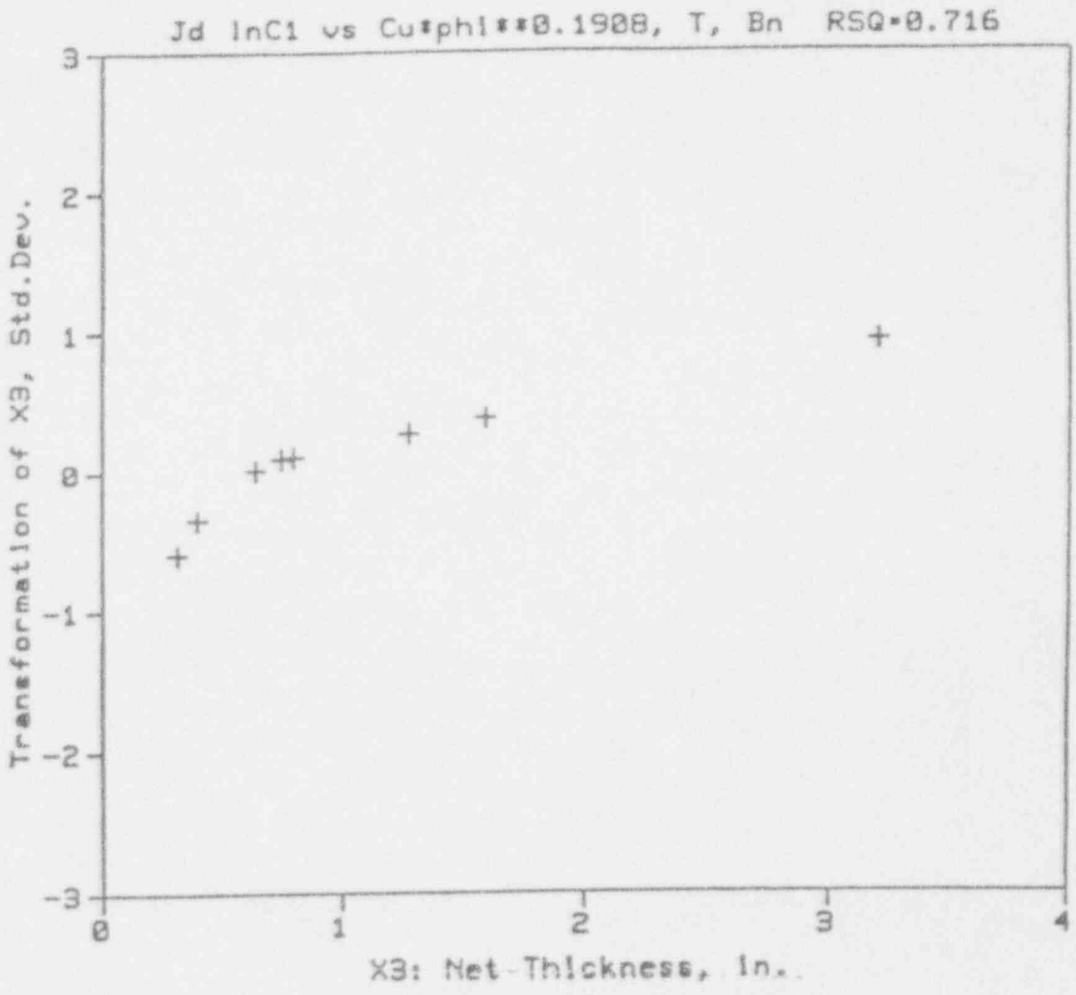

Figure B-12. TAP for Net Thickness on J_M

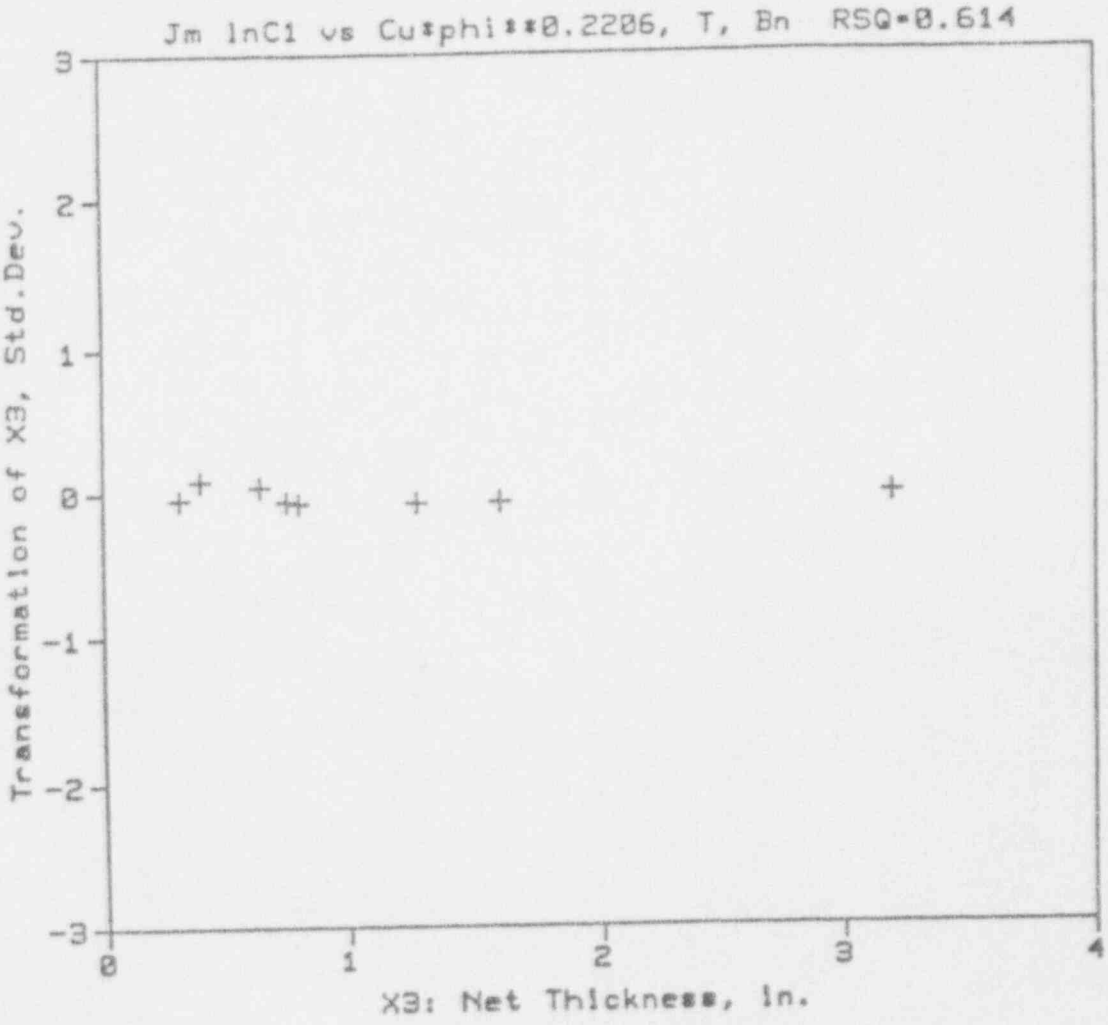

Figure B-13. Normalized J_D Plot - B&WOG Data

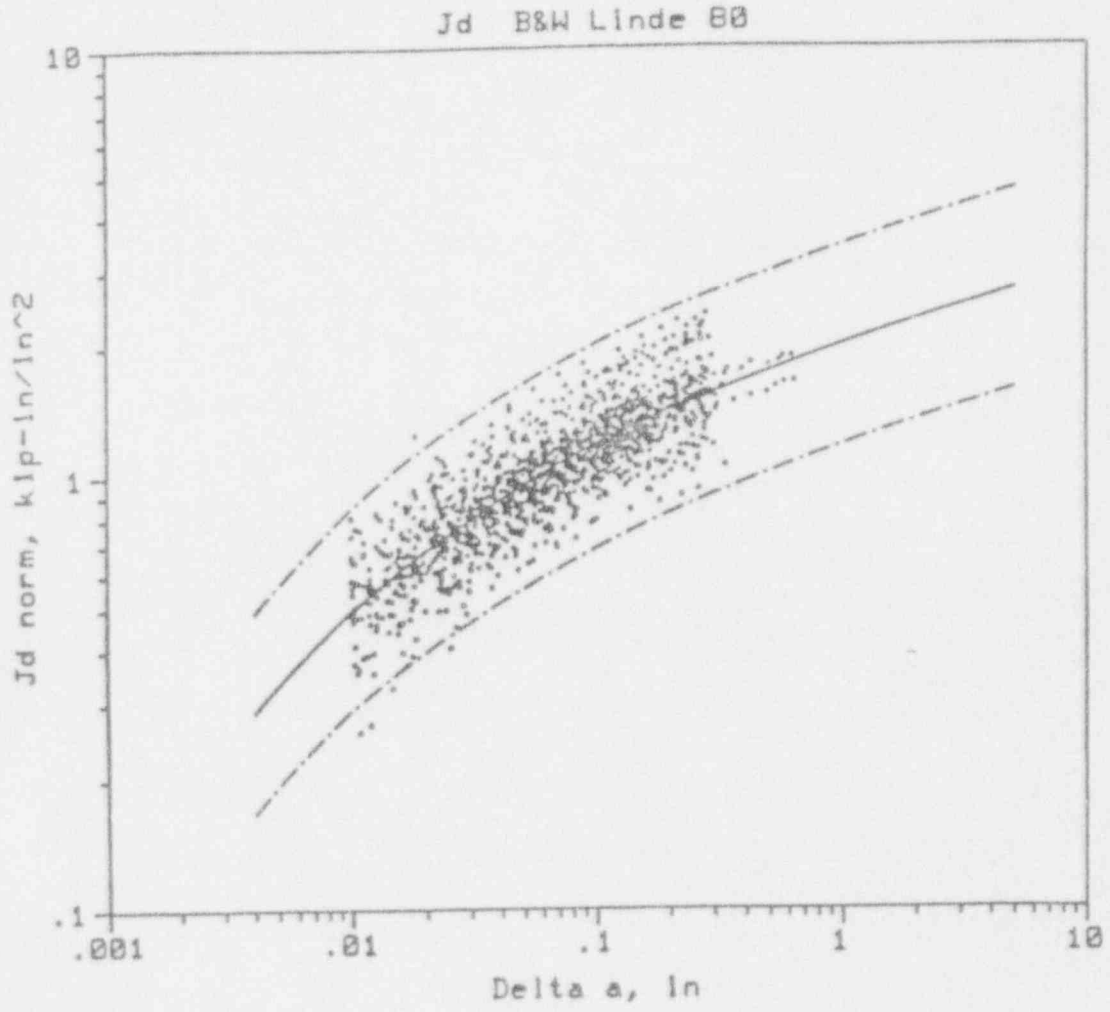

Figure B-14. Normalized J_M Plot - B&WOG Data

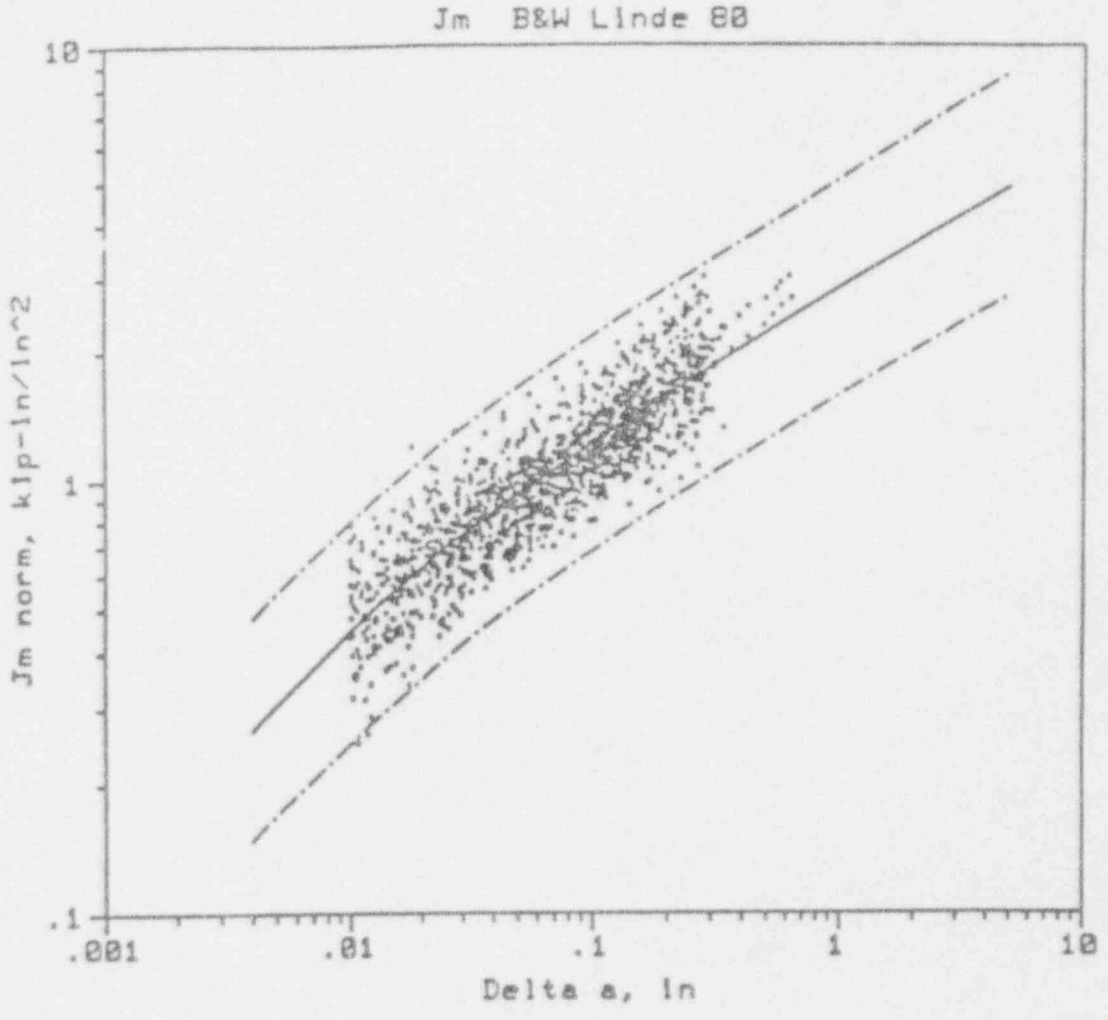

APPENDIX C

Location and Identification of Materials
in Reactor Vessels

In the following pages, cross sectional views of reactor vessels are provided with appropriate identification of the weld metals for all sixteen reactor vessels of RVWG.

Figure C-1. Reactor Vessel of Oconee Unit 1

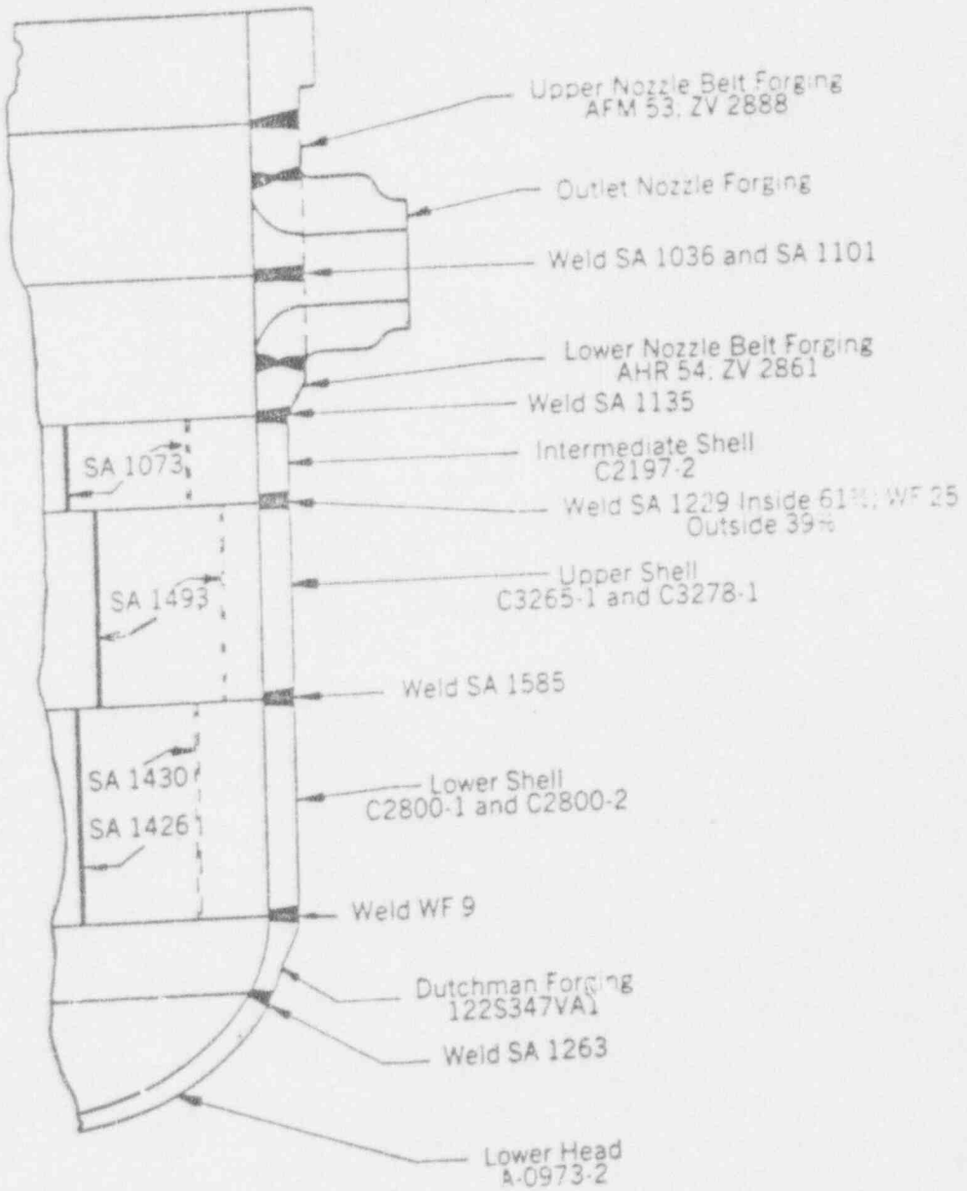

Figure C-2. Longitudinal Welds in Reactor Vessel of Oconee Unit 1

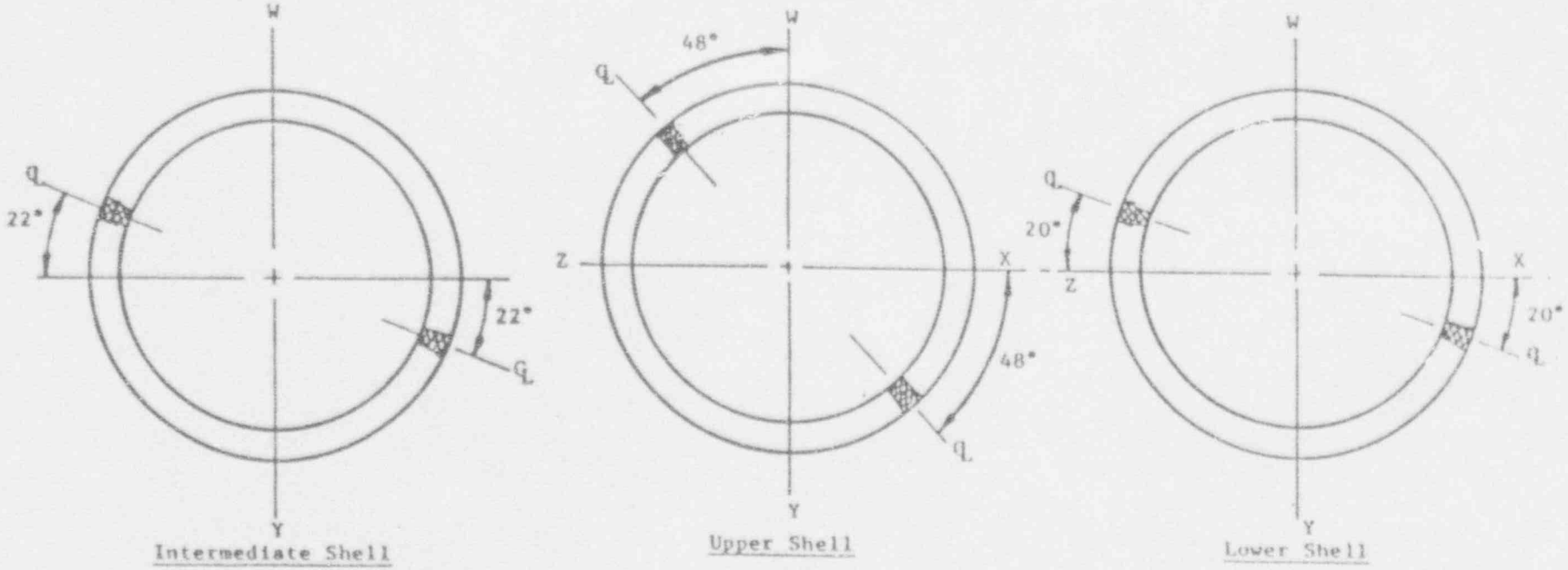

Figure C-3. Reactor Vessel of Oconee Unit 2

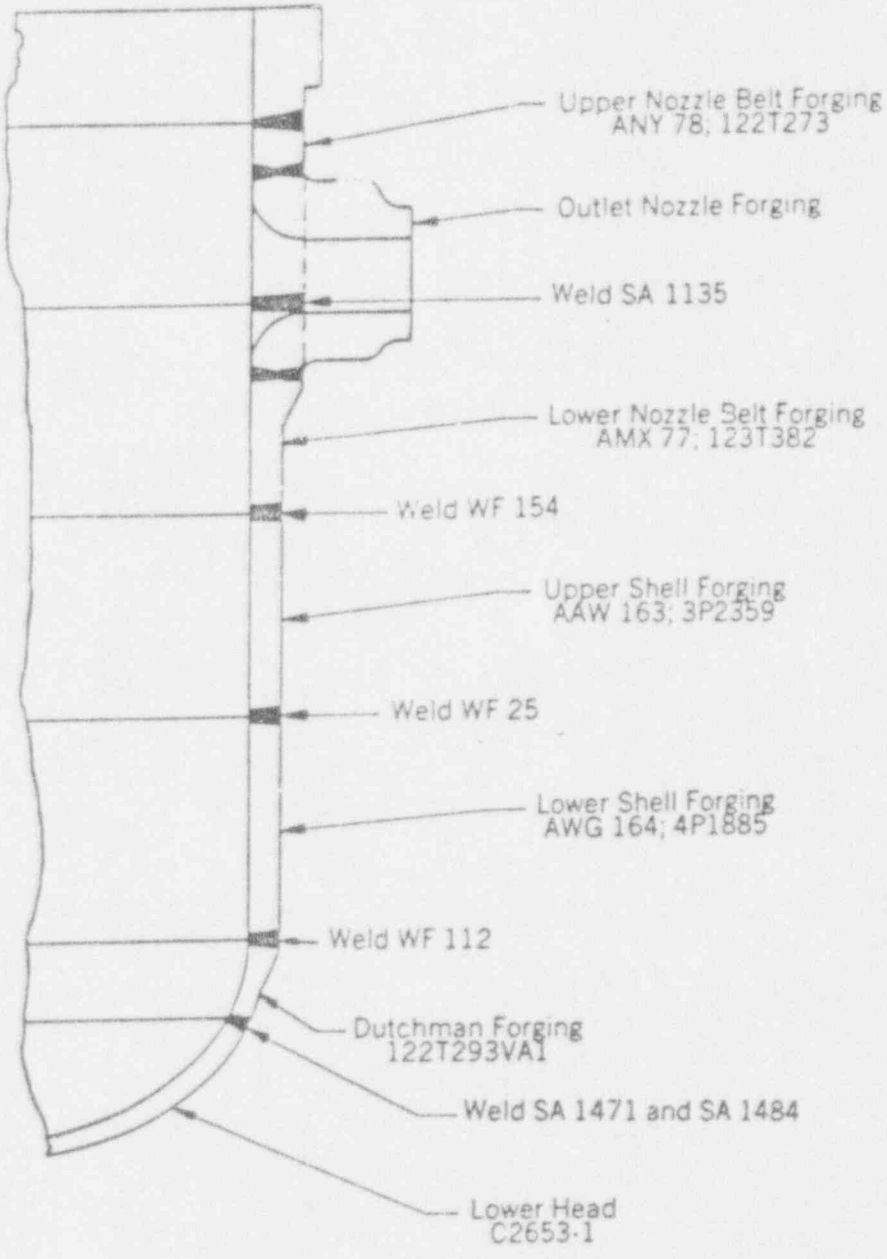

Figure C-4. Reactor Vessel of Oconee Unit 3

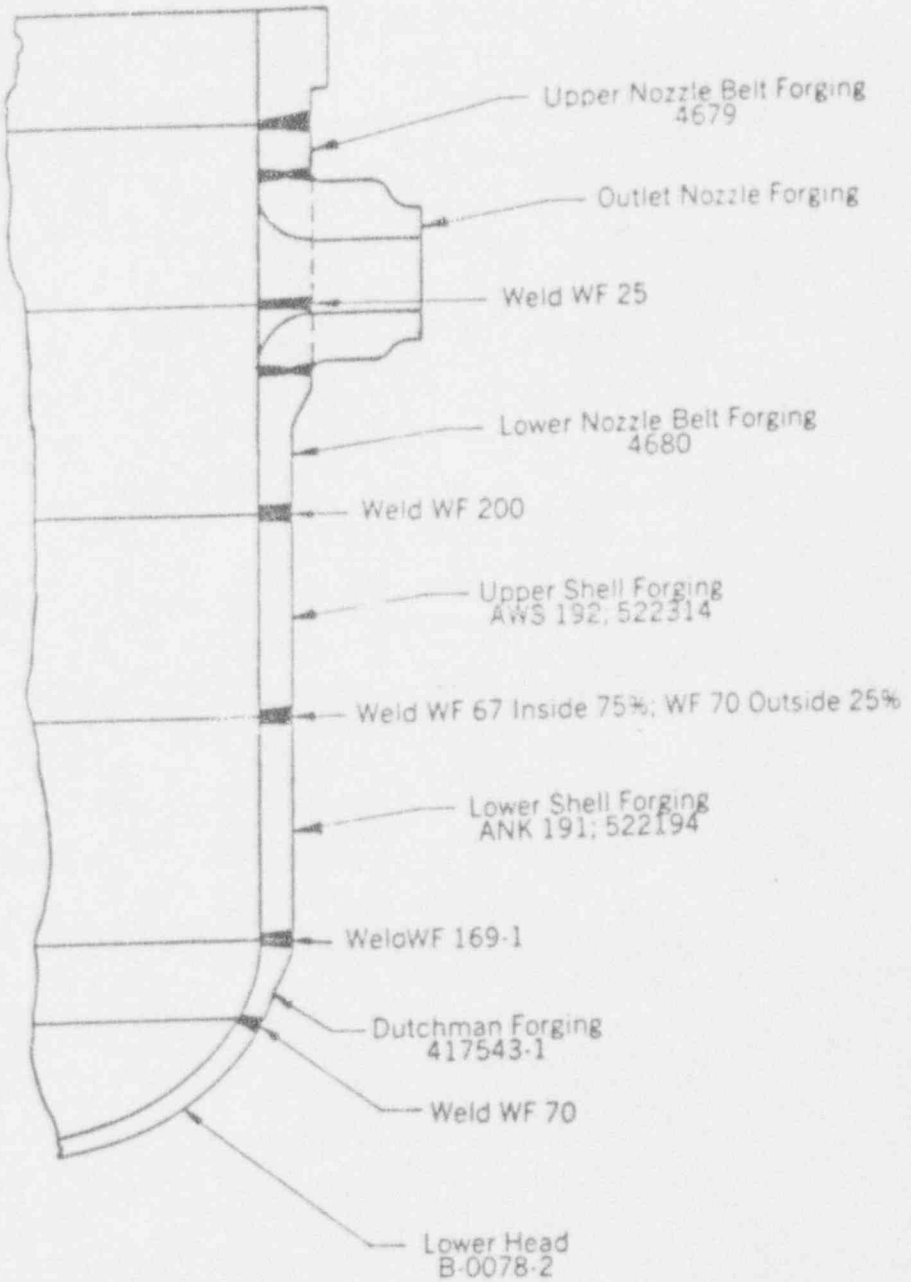

Figure C-5. Reactor Vessel of TMI-1

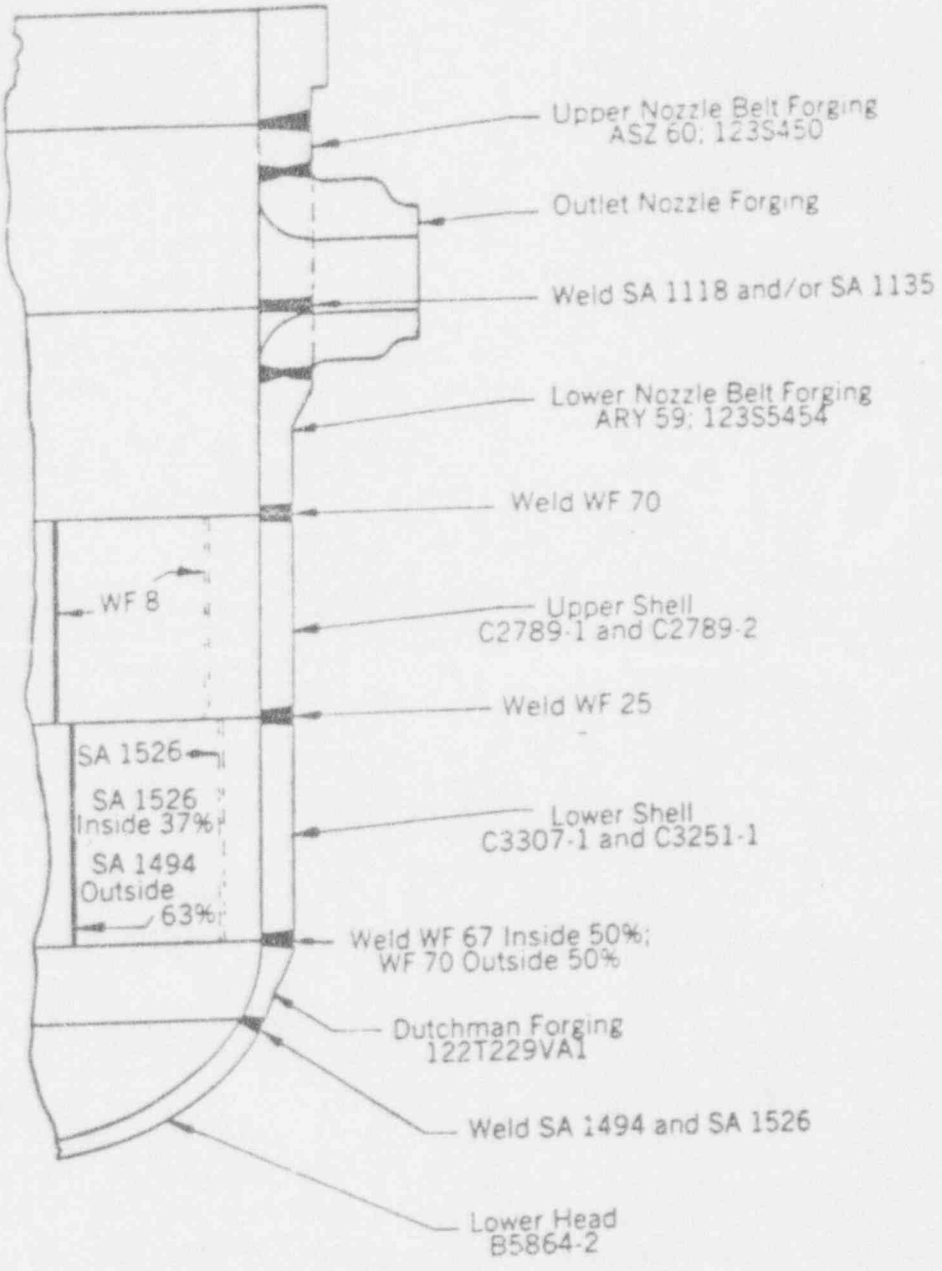

Figure C-6. Longitudinal Welds of TMI-1

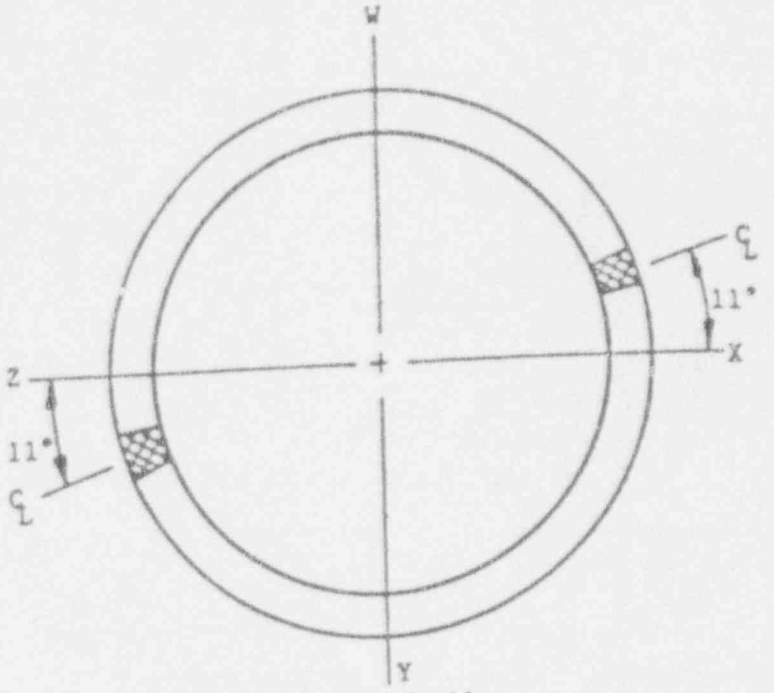

Upper Shell

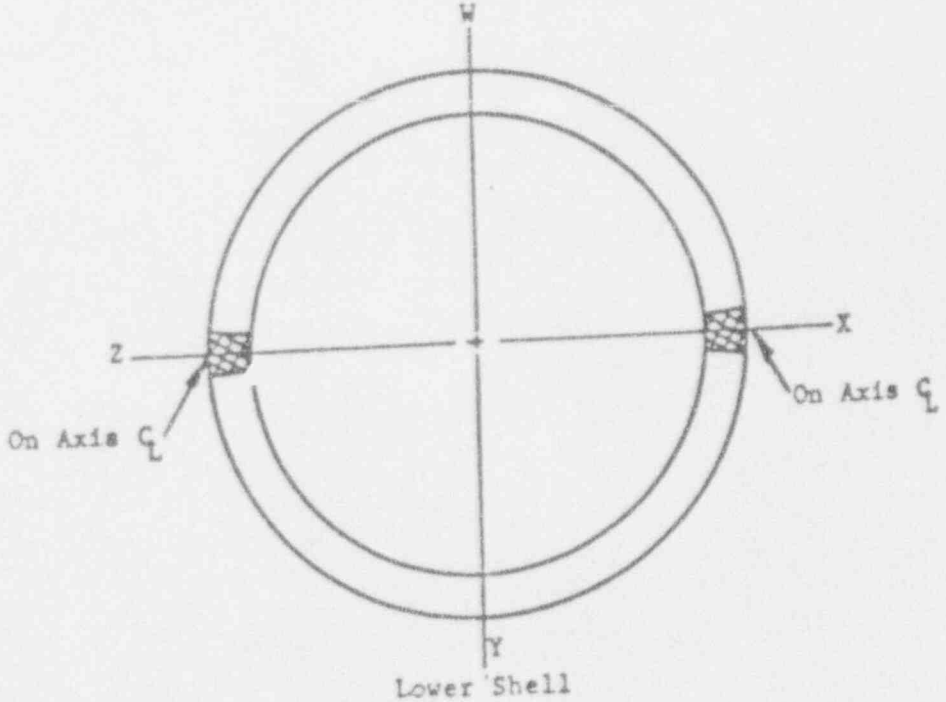

Lower Shell

Figure C-7. Reactor Vessel of Crystal River Unit 3

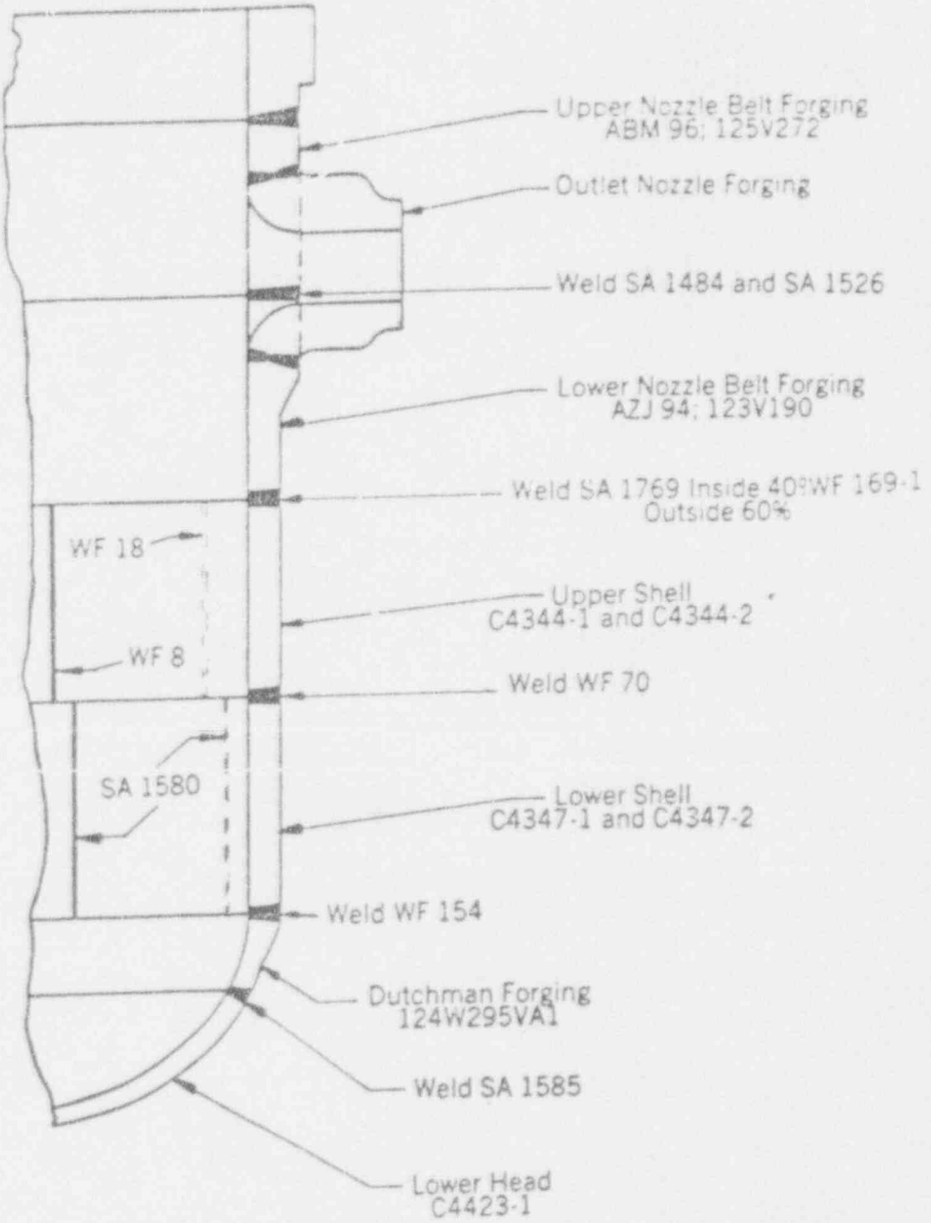

Figure C-8. Longitudinal Welds in Reactor Vessel of Crystal River Unit 3

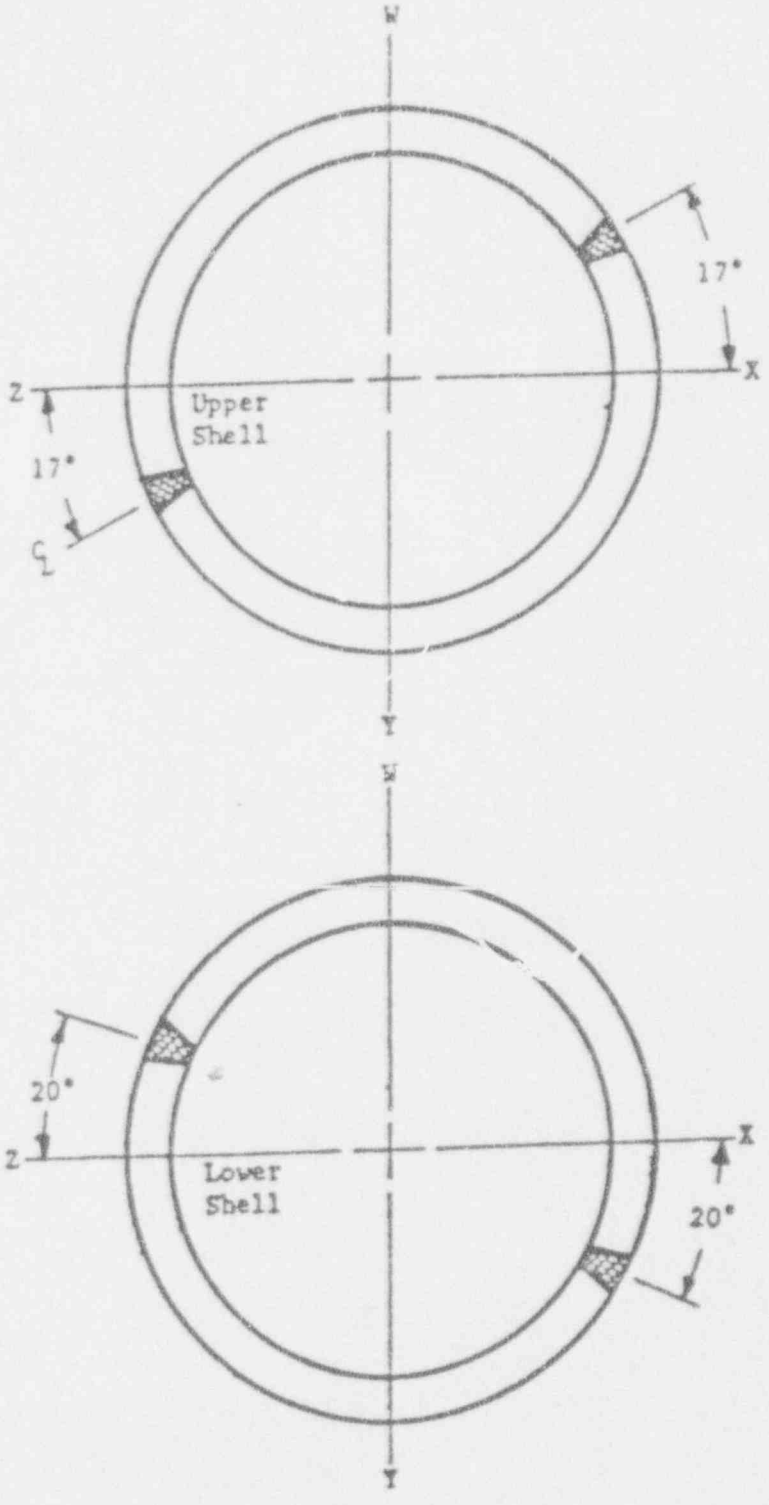

Figure C-9. Reactor Vessel of ANO-1

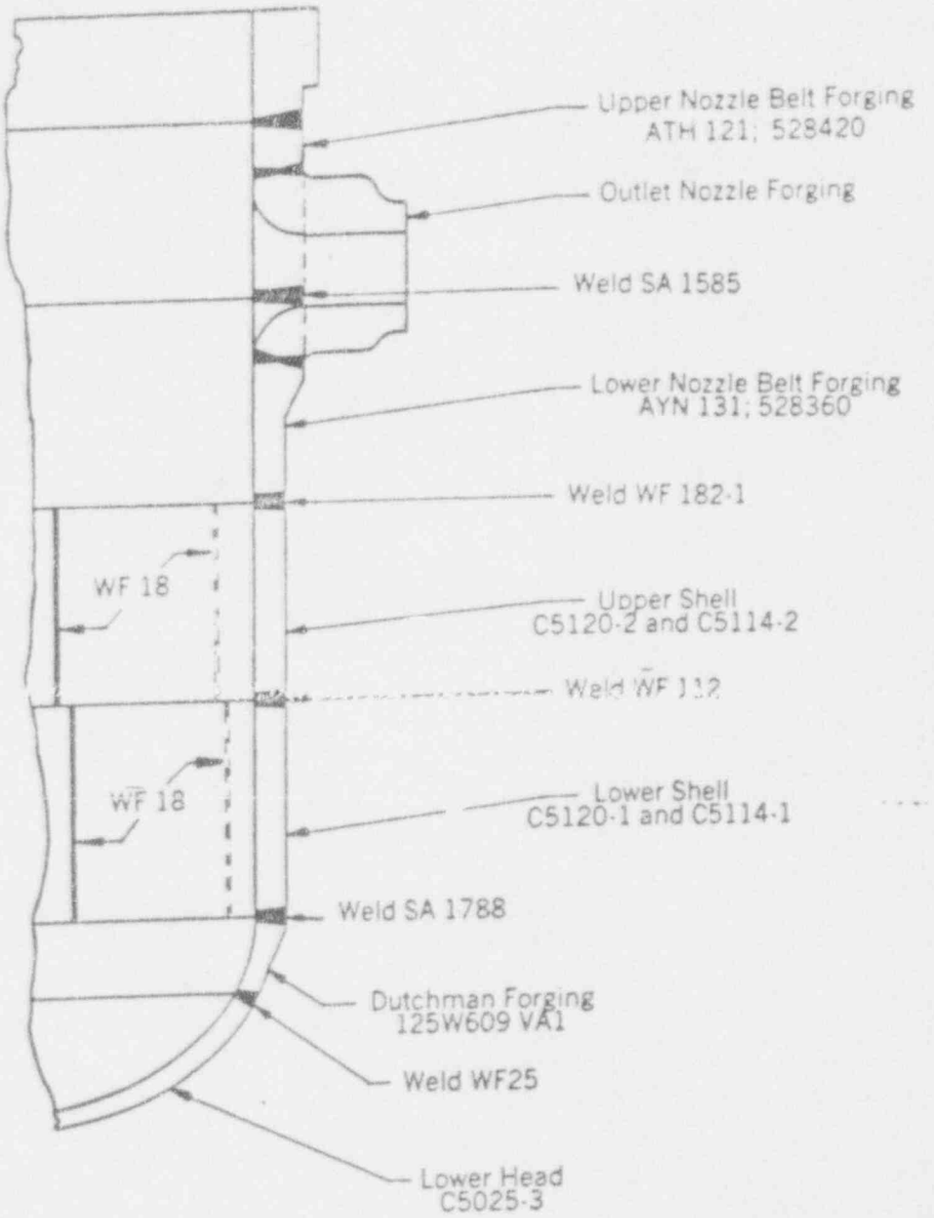

Figure C-10. Longitudinal Welds in Reactor Vessel of ANO-1

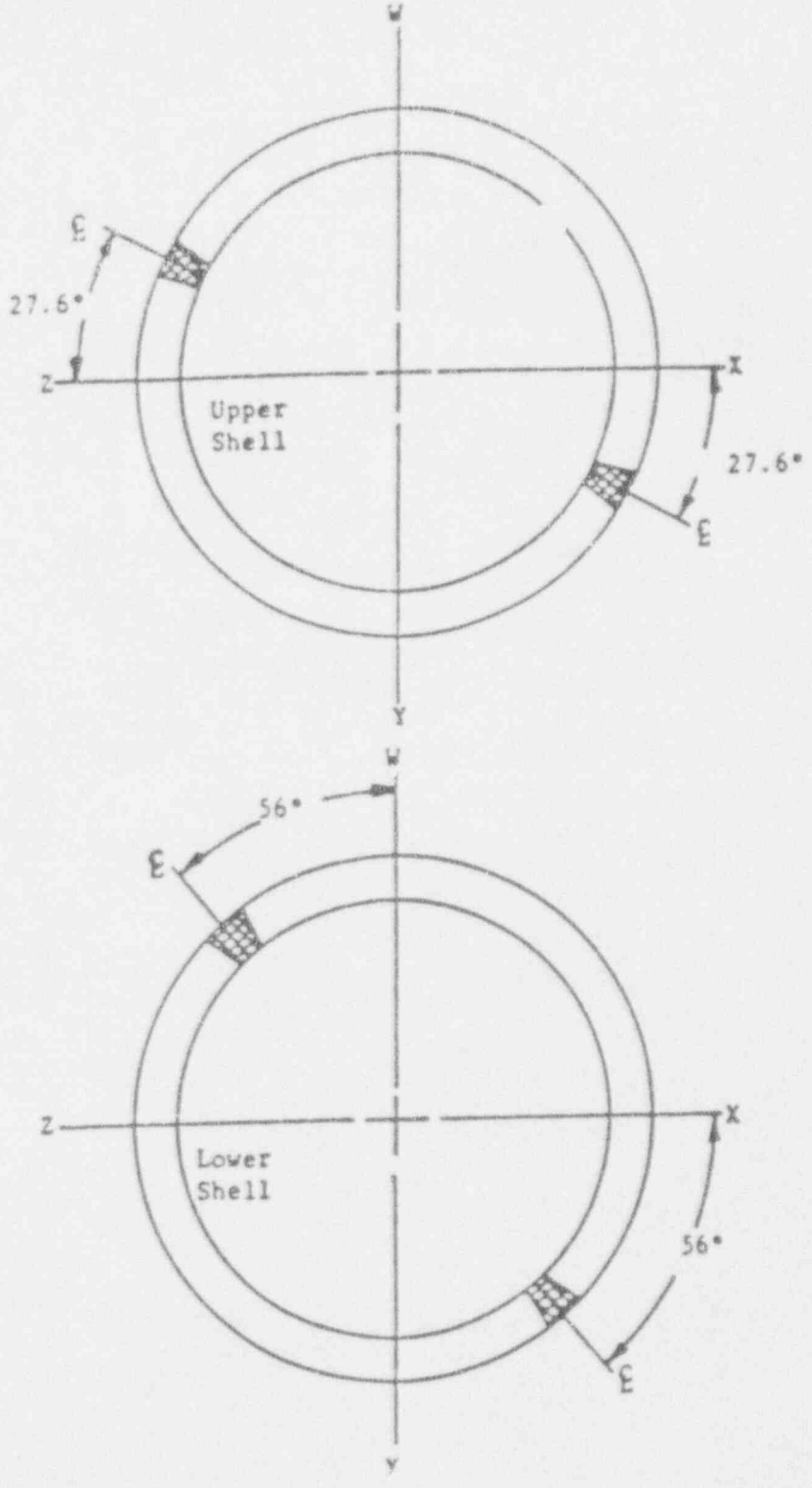

Figure C-11. Reactor Vessel of Davis-Besse Unit 1

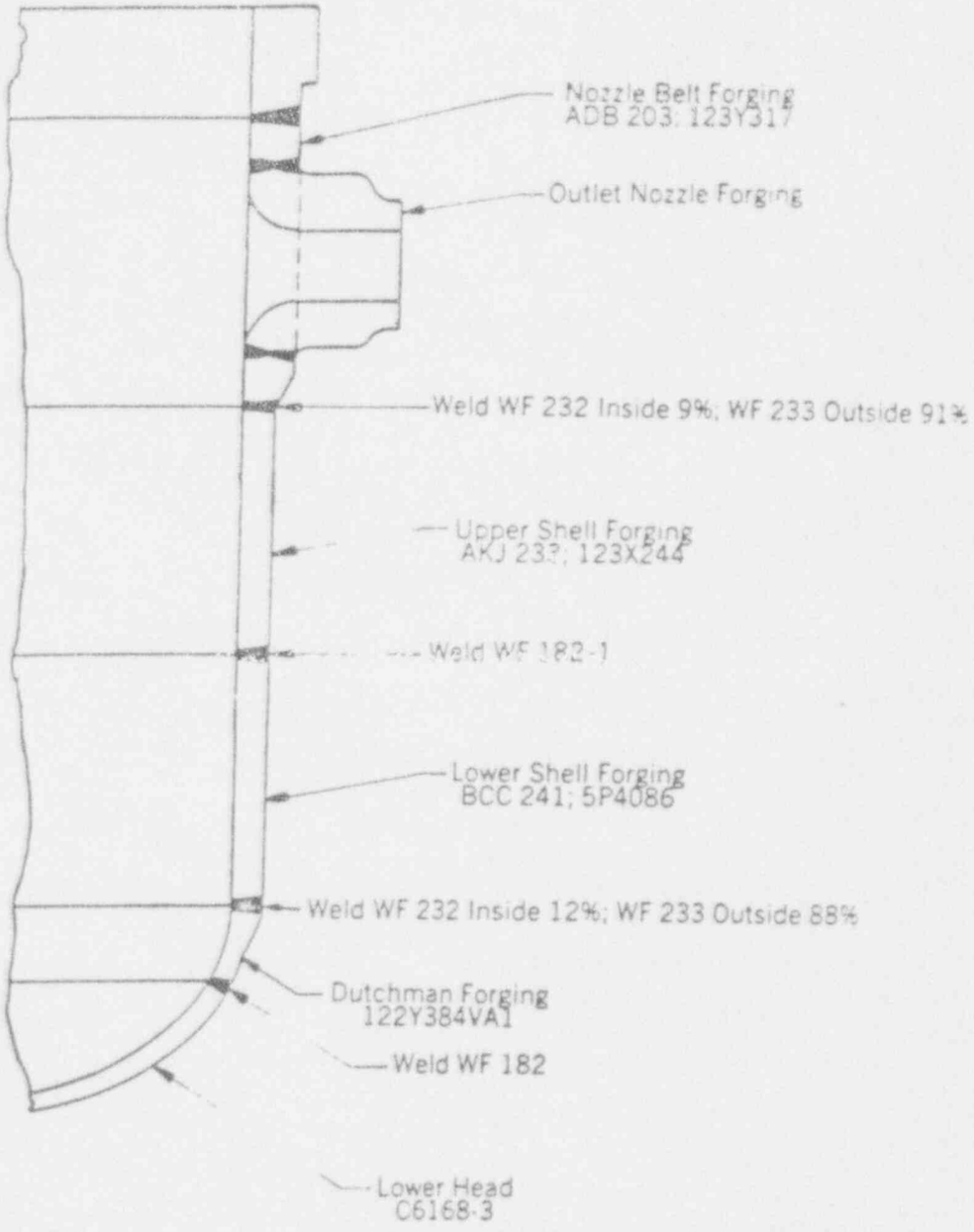

Figure C-12. Reactor Vessel of R. E. Ginna Unit 1

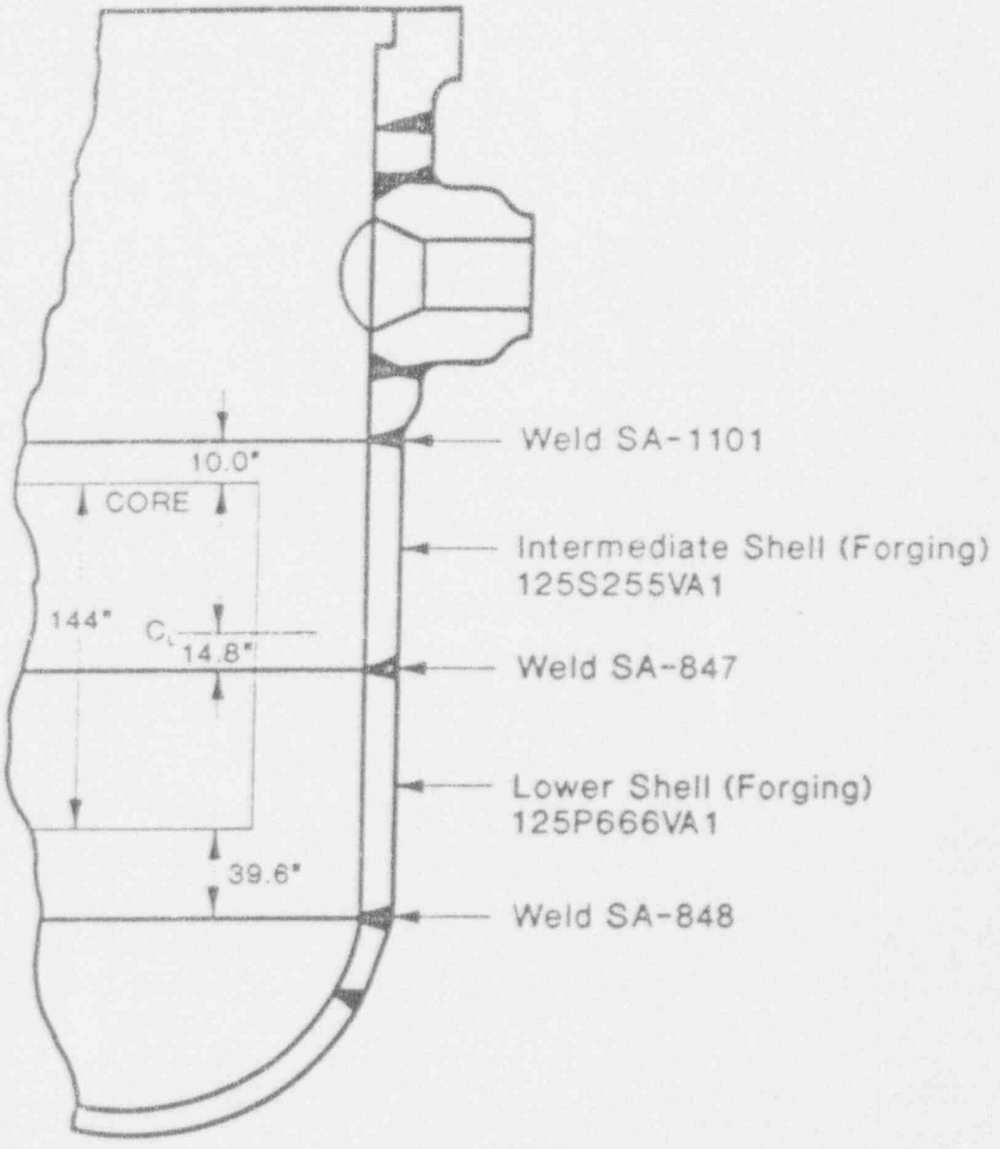

Figure C-13. Reactor Vessel of Point Beach Unit 1

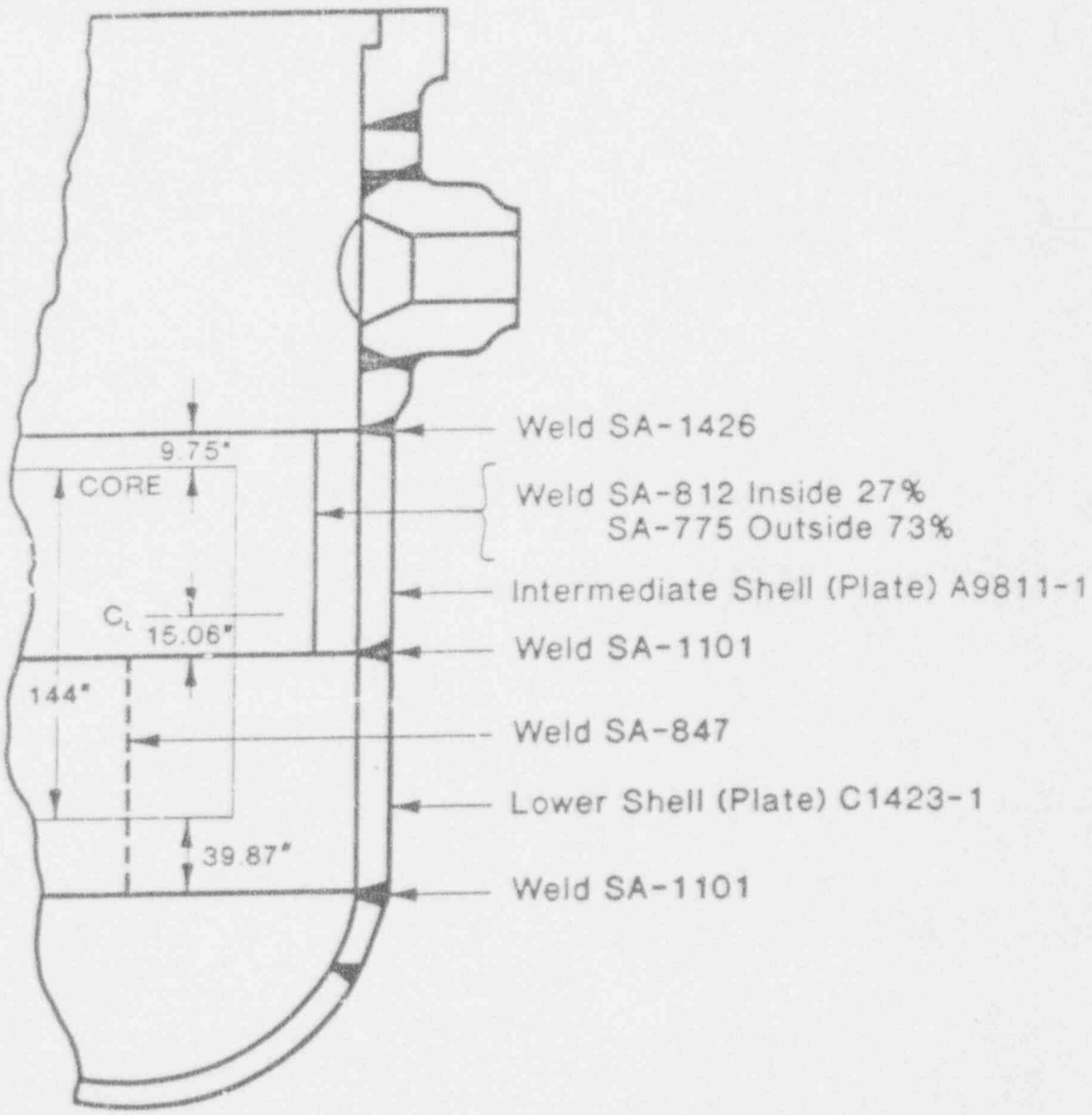

Figure C-14. Reactor Vessel of Point Beach Unit 2

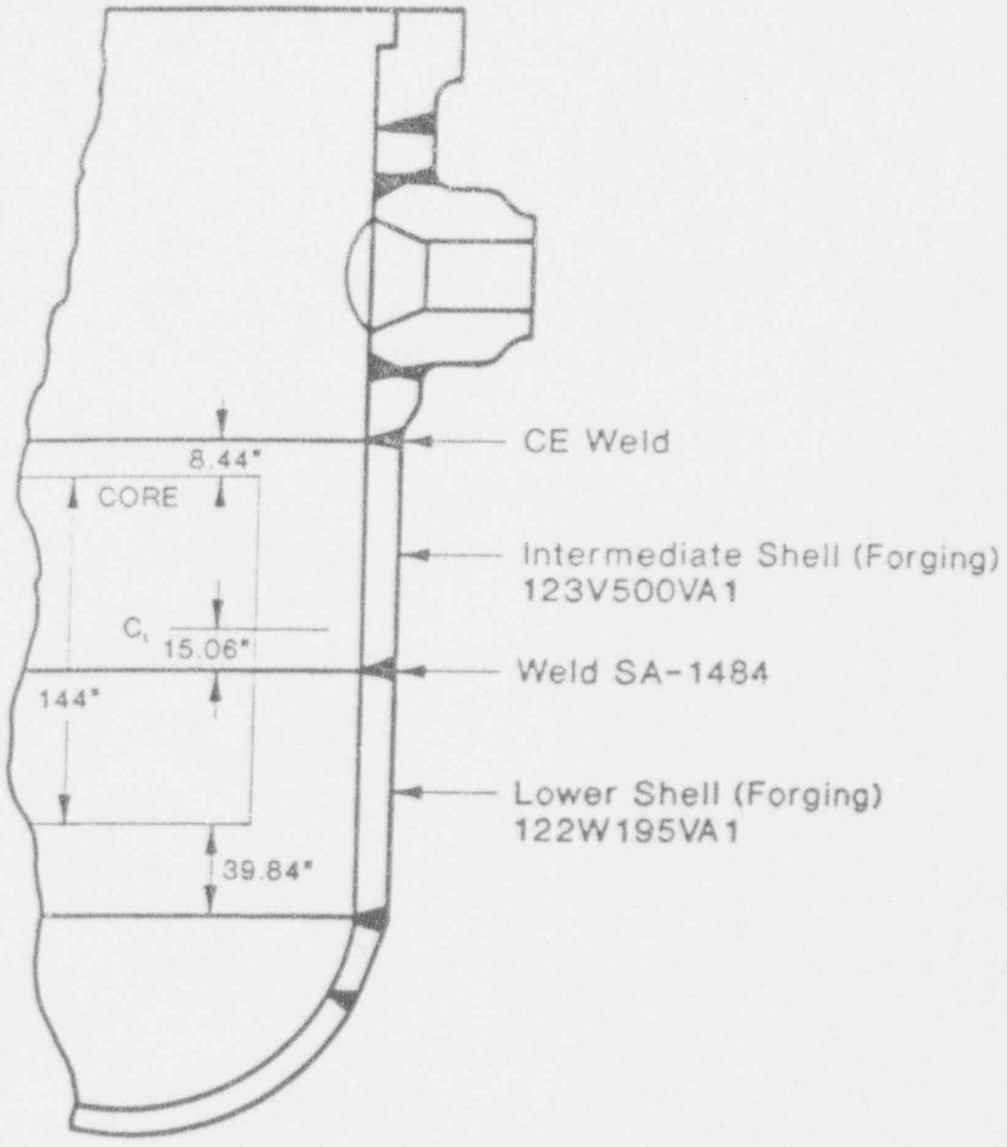

Figure C-15. Reactor Vessel of Surry Unit 1

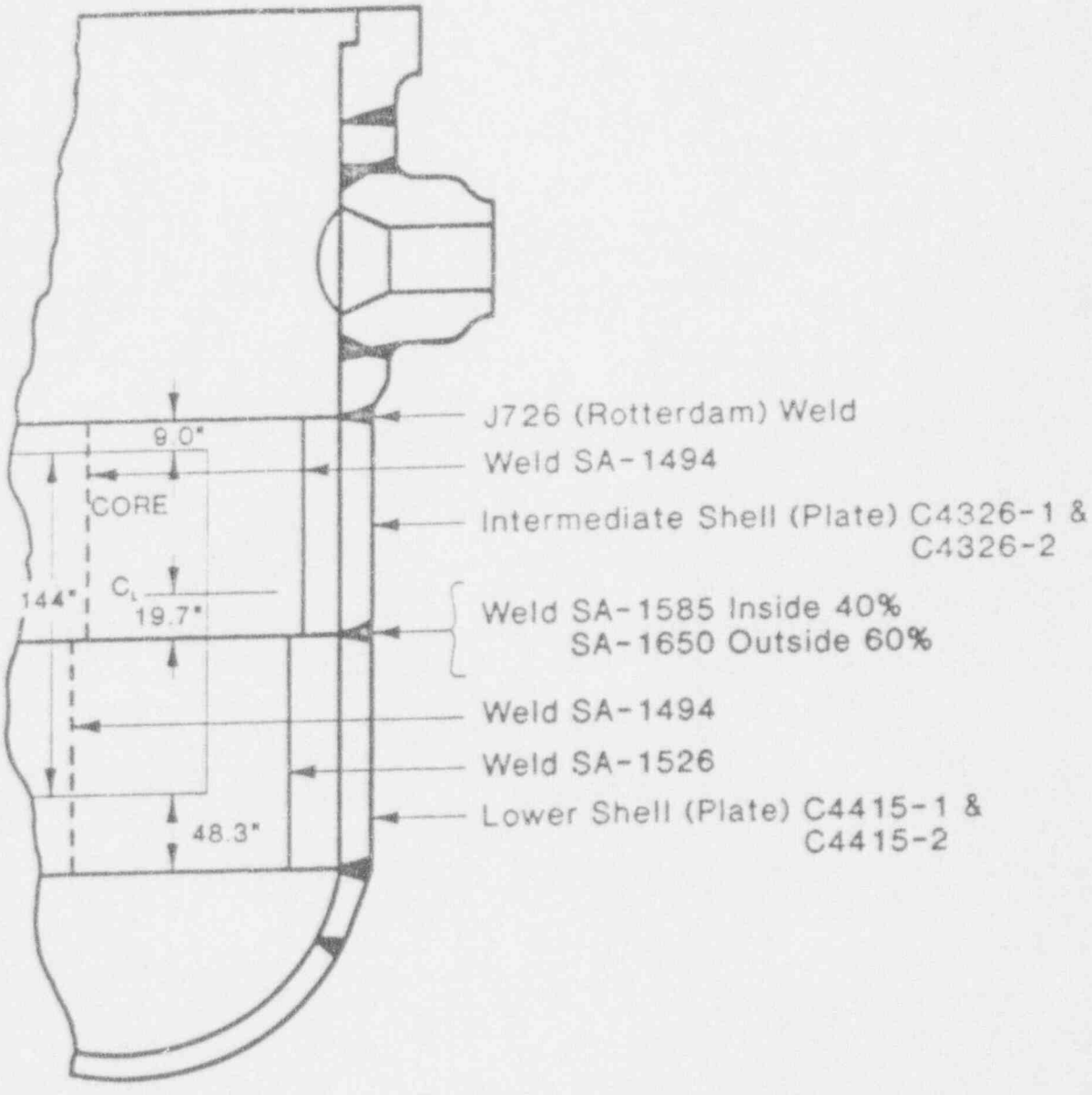

Figure C-16. Reactor Vessel of Surry Unit 2

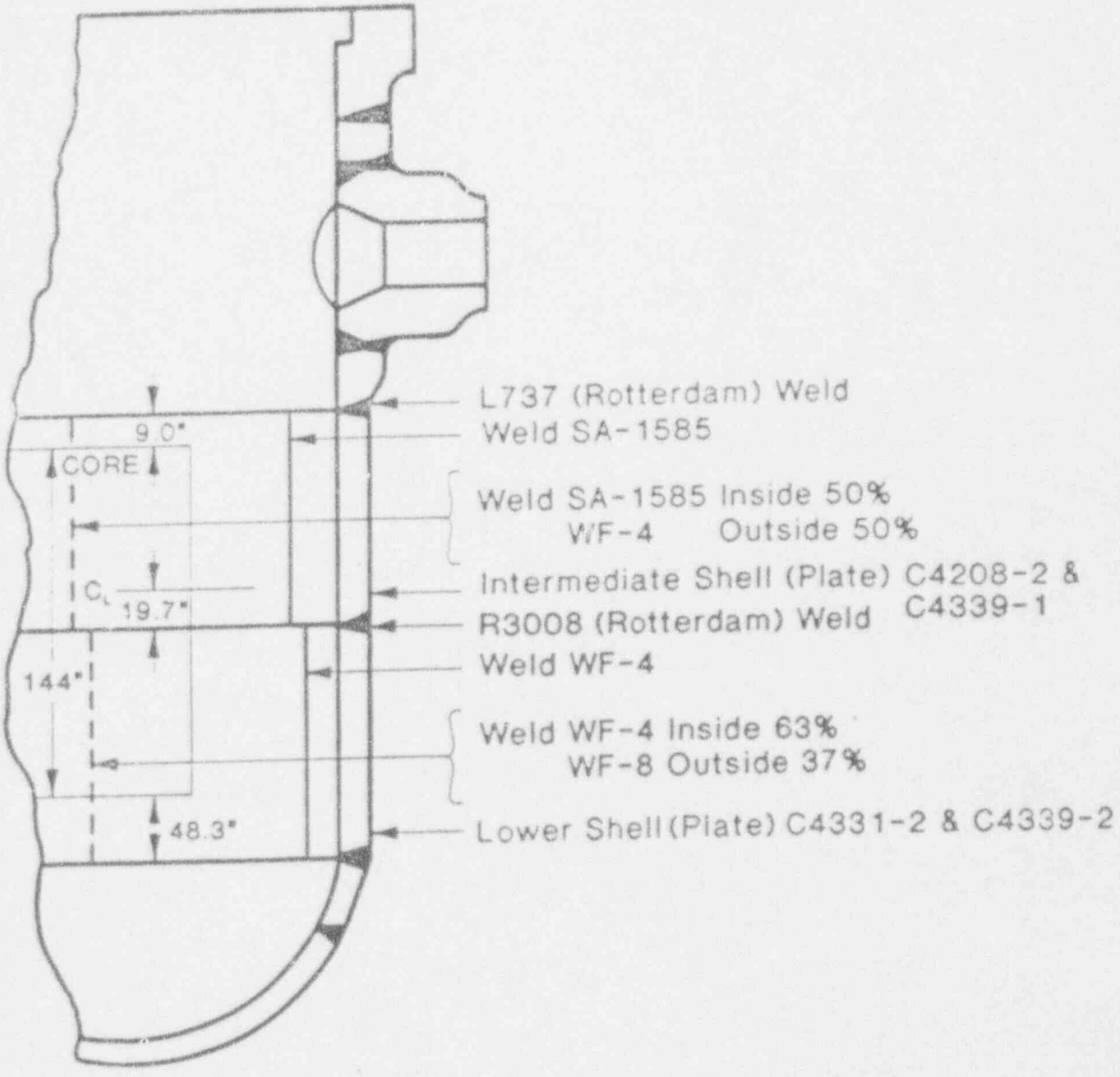

Figure C-17. Reactor Vessel of Turkey Point Unit 3

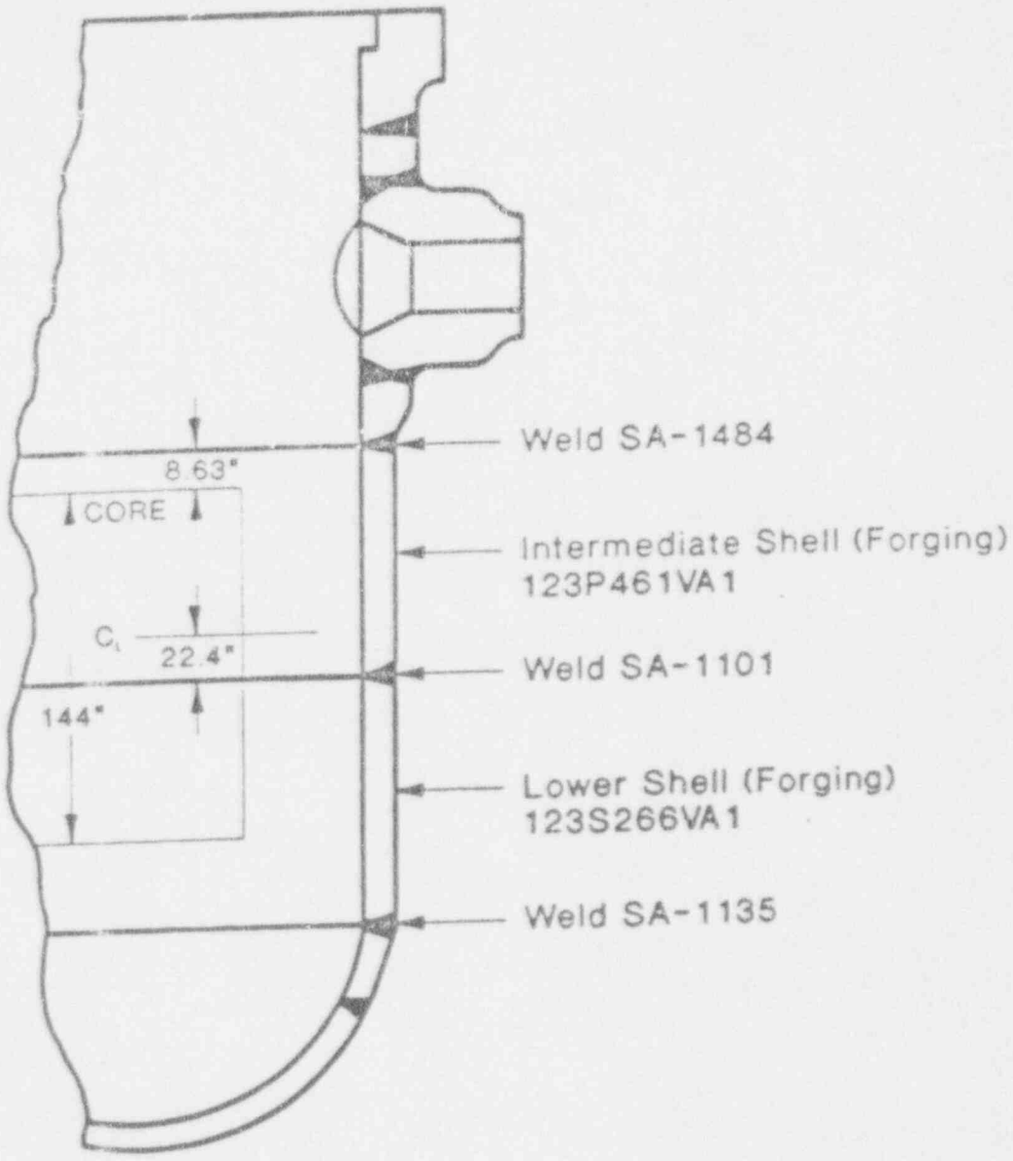

Figure C-18. Reactor Vessel of Turkey Point Unit 4

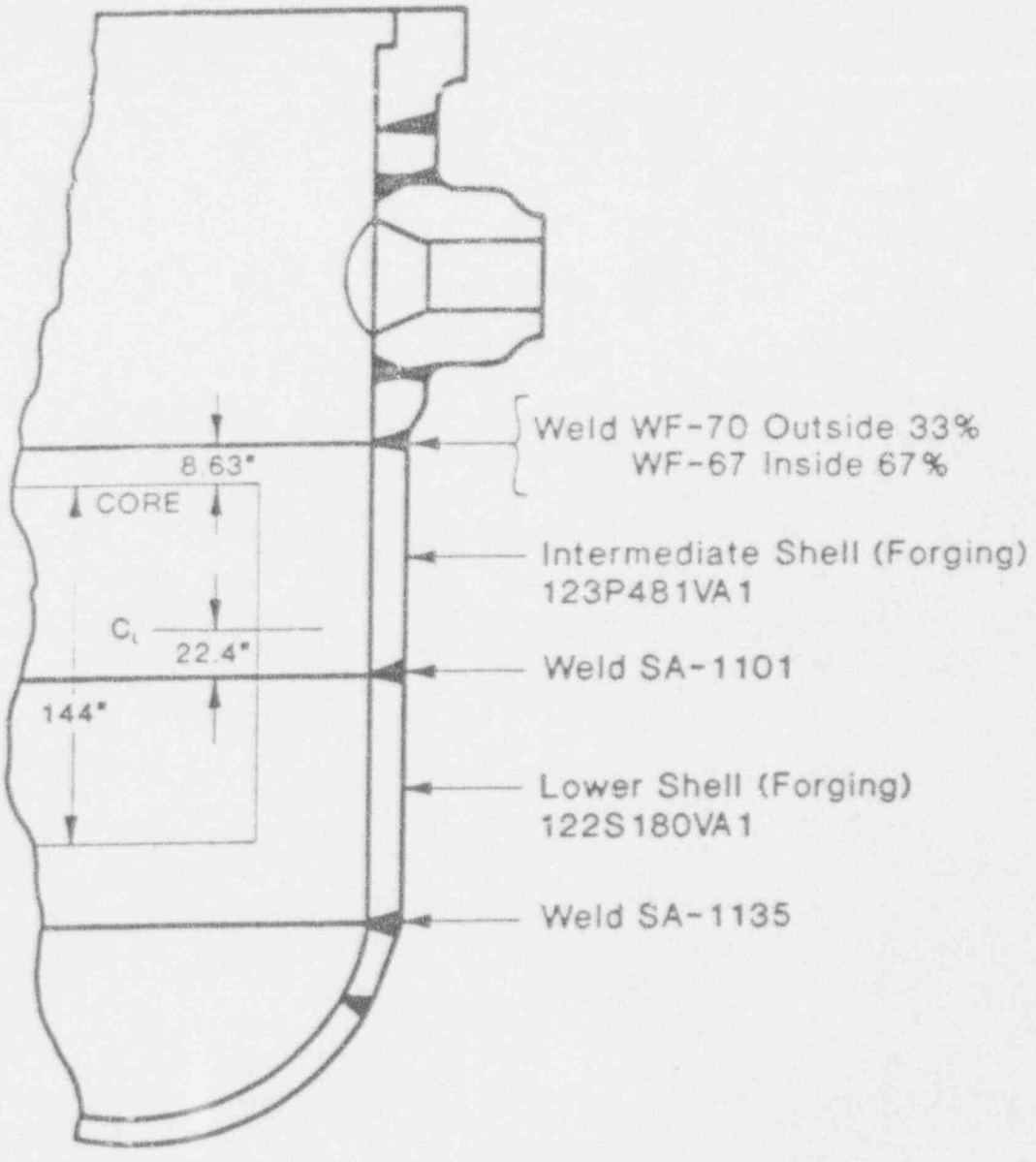

Figure C-19. Reactor Vessel of Zion Unit 1

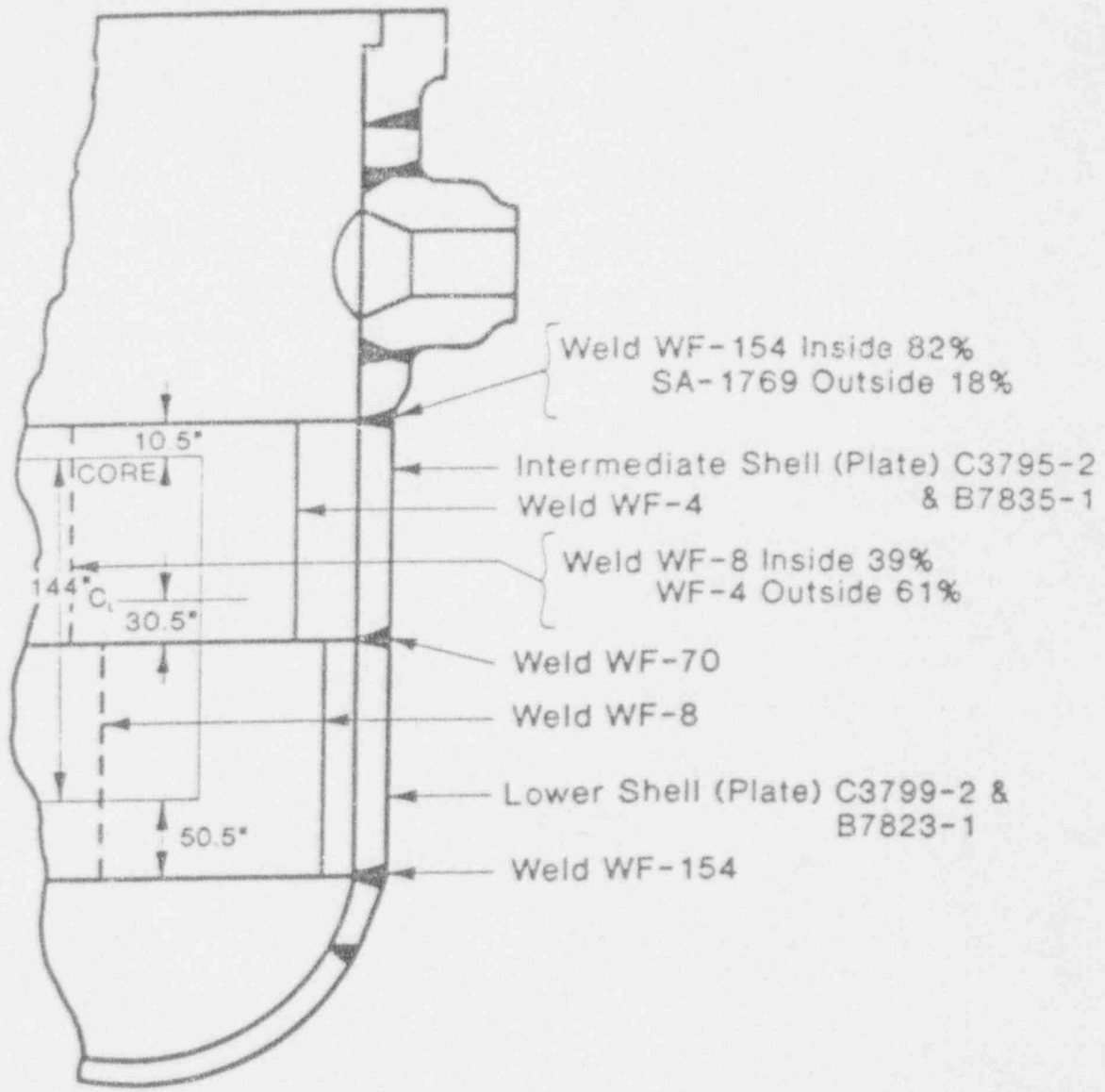

Figure C-20. Reactor Vessel of Zion Unit 2

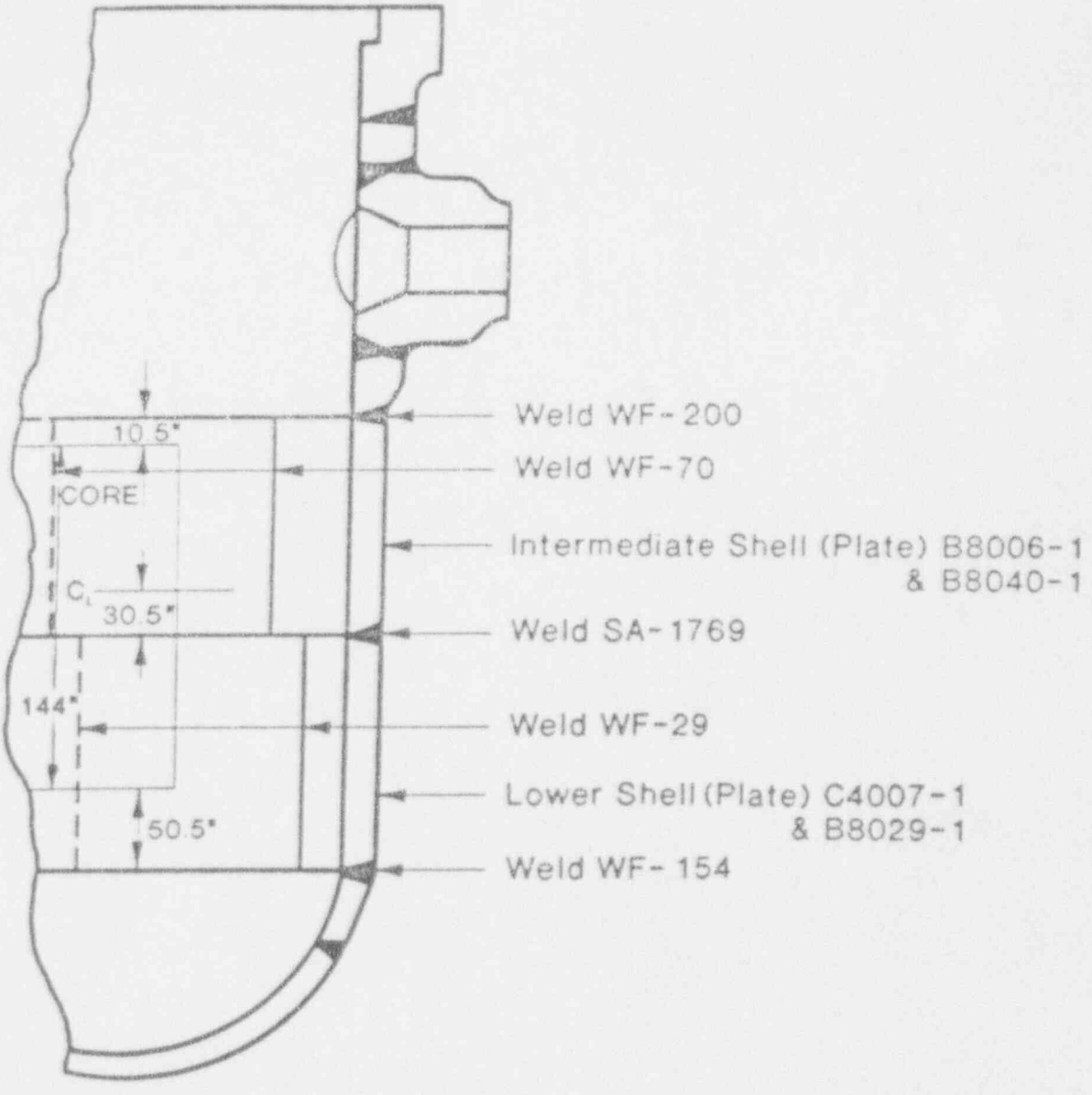

APPENDIX D

References for Appendices

1. Appendix G to Section III, "Nuclear Power Plant Components," of ASME Boiler and Pressure Vessel Code, New York (updated frequently).

2. BAW-10046A, Rev. 3, "Methods of Compliance with Fracture Toughness and Operational Requirements of 10CFR50, Appendix G," B&W Owners Group submitted to the NRC for approval, April 1990.

3. J. C. Newman, Jr. and I. S. Raju, "Stress-Intensity Factors for Internal Surface Cracks in Cylindrical Pressure Vessels," ASME Journal of Pressure Vessel Technology, Vol. 102, November 1980, pp. 342-346.

4. J. M. Bloom, "Extension of the Failure Assessment Diagram Approach - Semi-Elliptical Flaw in Pressurized Cylinder," ASME Journal of Pressure Vessel Technology, Vol. 107, February 1985.

5. V. Kumar, M. D. German and B. I. Schumacher, "Analysis of Elastic Surface Cracks in Cylinders Using the Line-Spring Model and Shell Finite Element Method," J of Pressure Vessel Technology, Vol. 107, November 1985.

6. V. Kumar and M. D. German, "Elastic-Plastic Fracture Analysis of Through-Wall and Surface Flaws in Cylinders," EPRI Report NP-5596, January 1988.

7. J. M. Bloom, "Procedure for the Assessment of the Integrity of Nuclear Pressure Vessels and Piping Containing Defects," EPRI Report NP-2431, June 1982, Appendix B.

8. E. D. Eason and E. E. Nelson, Improved Model for Predicting J-R Curves from Charpy Data, NUREG/CR 5356, Phase I Final Report, April 1989.

9. E. D. Eason et al., "Multivariable Modeling of Pressure Vessel and Piping J-R Data," SBIR Phase II Final Report," Modeling Computing Services, April 1991.

10. L. Breiman and J. H. Friedman, "Estimating Optimal Transformations for Multiple Regression and Correlation," J. American Statistical Association, Vol. 80, No. 391, September 1985, pp. 580-619.

11. M. J. Powell, "A Method for Minimizing a Sum of Squares of Nonlinear Functions Without Calculating Derivatives," Computer Journal, Vol. 7, p. 303, 1965.

12. U.S. Code of Federal Regulations, Title 10, Energy, Part 50, Section 61, "Fracture Toughness Requirements for Protection Against Pressurized Thermal Shock Events," First Published - Fedral Register, Vol. 50, No. 141, July 23, 1985.

13. ASTM Standard E1152-87, Standard Test Method for Determining J-R Curves, American Society for Testing and Materials, Philadelphia, Penn.

14. J. A. Joyce and E. M. Hackett, "Development of an Engineering Definition of the Extent of J Singularity Controlled Crack Growth," NUREG/CR-5238, U.S. Nuclear Regulatory Commission, May 1989.